

## Large Elastic Deformations of Isotropic Materials. VII. Experiments on the Deformation of Rubber

R. S. Rivlin and D. W. Saunders

*Phil. Trans. R. Soc. Lond. A* 1951 **243**, 251-288

doi: 10.1098/rsta.1951.0004

### Email alerting service

Receive free email alerts when new articles cite this article - sign up in the box at the top right-hand corner of the article or click [here](#)

To subscribe to *Phil. Trans. R. Soc. Lond. A* go to: <http://rsta.royalsocietypublishing.org/subscriptions>

## LARGE ELASTIC DEFORMATIONS OF ISOTROPIC MATERIALS

## VII. EXPERIMENTS ON THE DEFORMATION OF RUBBER

By R. S. RIVLIN

*Davy Faraday Laboratory of the Royal Institution*

AND D. W. SAUNDERS

*British Rubber Producers' Research Association**(Communicated by E. N. da C. Andrade, F.R.S.—Received 4 September 1950)*

## CONTENTS

	PAGE		PAGE
1. Introduction	252	16. Results of the experiment on simple torsion	277
A. EXPERIMENTS ON PURE HOMOGENEOUS DEFORMATION	255	17. The experiments on combined torsion and simple extension	280
2. Theoretical considerations	255	18. Experimental results	281
3. The experimental arrangement	257	19. Discussion	284
4. Experimental results	259	D. APPENDICES	285
5. Experiments at low values of $I_1$ and $I_2$	263	20. Appendix I. The preparation of the vulcanized rubber specimens	285
6. Experiment on pure shear	264	21. Appendix 2. The Mooney form of the stored-energy function	285
7. Experiment on pure shear superposed on simple extension	265	22. Appendix 3. Preliminary experiment on the method of measuring the forces in the experiments on pure homogeneous deformation	286
8. Experimental results	266	23. Appendix 4. The linearity of the relation between $[\partial W/\partial I_1 + (1/\lambda) \partial W/\partial I_2]$ and $1/\lambda$ for simple extension	287
9. Experiment on simple extension	268	24. Appendix 5. Further remarks on the results of the simple compression experiment	287
10. Results of the experiment on simple extension	268	REFERENCES	288
B. EXPERIMENT ON COMPRESSION	270		
11. Theoretical considerations	270		
12. Description of the experiment	271		
13. Experimental results	273		
C. EXPERIMENTS ON THE TORSION OF A CYLINDER	275		
14. Basic formulae	275		
15. The experiment on simple torsion	276		

It is shown in this part how the theory of large elastic deformations of incompressible isotropic materials, developed in previous parts, can be used to interpret the load-deformation curves obtained for certain simple types of deformation of vulcanized rubber test-pieces in terms of a single stored-energy function.

The types of experiment described are:

- (i) the pure homogeneous deformation of a thin sheet of rubber in which the deformation is varied in such a manner that one of the invariants of the strain,  $I_1$  or  $I_2$ , is maintained constant;
- (ii) pure shear of a thin sheet of rubber (i.e. pure homogeneous deformation in which one of the extension ratios in the plane of the sheet is maintained at unity, while the other is varied);

(iii) simultaneous simple extension and pure shear of a thin sheet (i.e. pure homogeneous deformation in which one of the extension ratios in the plane of the sheet is maintained constant at a value less than unity, while the other is varied);

(iv) simple extension of a strip of rubber;

(v) simple compression (i.e. simple extension in which the extension ratio is less than unity);

(vi) simple torsion of a right-circular cylinder;

(vii) superposed axial extension and torsion of a right-circular cylindrical rod.

It is shown that the load-deformation curves in all these cases can be interpreted on the basis of the theory in terms of a stored-energy function  $W$  which is such that  $\partial W/\partial I_1$  is independent of  $I_1$  and  $I_2$  and the ratio  $(\partial W/\partial I_2)/(\partial W/\partial I_1)$  is independent of  $I_1$  and falls, as  $I_2$  increases, from about 0.25 at  $I_2 = 3$ .

## 1. INTRODUCTION

In the earlier parts (Rivlin 1948*a, b, c, d*; 1949*a, b*) a mathematical theory has been developed which describes the deformation, under the action of applied forces, of bodies of ideal highly elastic materials which are incompressible and isotropic in their undeformed state. The relevant physical properties of the material are specified in terms of a stored-energy function  $W$  which must be a function of two strain invariants  $I_1$  and  $I_2$ .

These invariants are expressible in terms of the principal extension ratios  $\lambda_1$ ,  $\lambda_2$  and  $\lambda_3$  at the point of the deformed body considered, by the formulae

$$I_1 = \lambda_1^2 + \lambda_2^2 + \lambda_3^2 \quad \text{and} \quad I_2 = \frac{1}{\lambda_1^2} + \frac{1}{\lambda_2^2} + \frac{1}{\lambda_3^2}, \quad (1.1)$$

in which, since the material of the body is assumed incompressible,  $\lambda_1 \lambda_2 \lambda_3 = 1$ .

From the theory it has been found possible to calculate the forces necessary to produce certain simple types of deformation in bodies of simple form, in terms of  $W$  (generally through its derivatives  $\partial W/\partial I_1$  and  $\partial W/\partial I_2$ ) and parameters describing the amount of deformation. Among the deformations for which the appropriate forces have been calculated are:

(i) the pure homogeneous deformation of a sheet, the major surfaces of which are force-free (simple extension and pure shear are particular cases of this deformation);

(ii) torsion of a right-circular cylinder and torsion of a right-circular cylinder which is subjected to a preliminary simple extension.

These results can be used for experimental purposes in two ways. Knowing the form of  $W$  as a function of  $I_1$  and  $I_2$  for a particular material, the forces necessary to produce specified deformations can be explicitly calculated and the results compared with experiments carried out on appropriate test-pieces of the material. Alternatively, the results of experiments carried out on test-pieces of the material can be used in order to give some information regarding the dependence of  $W$  on  $I_1$  and  $I_2$  for the material of which the test-pieces are made.

It will be noted that when the material is undeformed  $\lambda_1 = \lambda_2 = \lambda_3 = 1$ , so that  $I_1 = I_2 = 3$ . It is therefore convenient for some purposes to consider the stored-energy function to have the form of a doubly-infinite series in  $(I_1 - 3)$  and  $(I_2 - 3)$  thus:

$$W = \sum_{i=0, j=0}^{\infty} C_{ij} (I_1 - 3)^i (I_2 - 3)^j, \quad C_{00} = 0. \quad (1.2)$$

It can be shown (see §21) that for small deformations  $(I_1 - 3)$  and  $(I_2 - 3)$  are, in general, small quantities of the same order, so that, whatever may be the form of  $W$ , the expression

$$W = C_{10}(I_1 - 3) + C_{01}(I_2 - 3), \quad (1.3)$$

represents an approximation, valid for sufficiently small deformations. It has been shown by Mooney (1940) that this form for  $W$  is the most general one which can be valid, even for large deformations, for an ideal incompressible highly elastic material, isotropic in its undeformed state, if the relation between the shearing force and amount of simple shear is linear, when the material is subjected to a simple shear superposed on a constant simple extension. The form (1.3) for the stored-energy function will accordingly be referred to as the Mooney form.

It is the object of the present paper to show how the theory of large elastic deformations can be used to explain the load-deformation characteristics of vulcanized rubber for certain simple types of deformation in terms of a single form of stored-energy function. This task is made more difficult than it otherwise would be by the fact that some of the test-pieces used have to be moulded individually, and it is difficult to make two rubber specimens having identical properties even if nominally identical procedures are followed in preparing them.

In the first series of experiments (§§ 2 to 4) the forces necessary to produce various pure homogeneous deformations, for which either  $I_1$  or  $I_2$  have specified values, in a sheet of rubber are measured. From these measurements the values of  $\partial W/\partial I_1$  and  $\partial W/\partial I_2$  are found for various values of  $I_1$  and  $I_2$ . Unfortunately, the formulae which have to be employed, in order to calculate  $\partial W/\partial I_1$  and  $\partial W/\partial I_2$  from the measurements, greatly emphasize the experimental errors, and the values of  $\partial W/\partial I_1$  and  $\partial W/\partial I_2$  cannot be very accurately determined. It appears, however, that for the particular rubber employed,  $\partial W/\partial I_1$  is substantially independent of  $I_1$  and  $I_2$ , while  $\partial W/\partial I_2$  is independent of  $I_1$  and falls with increase of  $I_2$  from a value of about  $\frac{1}{8}\partial W/\partial I_1$  at  $I_2 = 5$  to about  $\frac{1}{24}\partial W/\partial I_1$  at  $I_2 = 30$ . These experiments have the desirable feature that  $I_1$  and  $I_2$  can, to a great extent, be varied independently of each other. Unfortunately, the magnification of the experimental error produced by the calculation makes the results too inaccurate to be of use for values of  $I_1$  and  $I_2$  below about 5.

In order to obtain some indication of the variation of  $W$  at lower values of  $I_1$  and  $I_2$  the experiments described in §§ 5 to 10 were carried out. In these, the load-deformation relations were obtained for pure shear, pure shear superposed on a constant simple extension, and simple extension. The three test-pieces used were cut from a single sheet of vulcanized rubber so that the results should be strictly comparable. In interpreting the experiments on pure shear, the assumption is made that  $\partial W/\partial I_1$  is still independent of  $I_1$  and  $I_2$ , that  $\partial W/\partial I_2$  depends on  $I_2$  only and that  $(\partial W/\partial I_2)/(\partial W/\partial I_1)$  has the same value at  $I_2 = 5$  as is obtained from the experiments described in §§ 2 to 4. It then appears that  $\partial W/\partial I_2$  falls steadily with increase in  $I_2$  from about  $\frac{1}{4}\partial W/\partial I_1$  at  $I_2 = 3$ , the rate of fall decreasing as  $I_2$  increases. The values of  $\partial W/\partial I_1$  and  $\partial W/\partial I_2$  found from the experiments on pure shear are used to predict the results of the experiments on simple extension and pure shear superposed on simple extension, good agreement being obtained.

In §§ 11 to 13 are described experiments carried out in simple extension and simple compression on test-pieces cut from a single sheet of vulcanized rubber, so that the results are strictly comparable. In §§ 14 to 19 are described experiments in which the forces required to produce simple torsion in a cylinder of vulcanized rubber and in a rod of similar material subjected to simple extension were measured as a function of the amount of torsion.

It is shown that all these experiments can be interpreted in terms of a stored-energy function  $W$  which varies with  $I_1$  and  $I_2$  in the manner indicated by the experiments described in §§ 2 to 10.

The theory on which the interpretation of the experiments is based was formulated for *ideal* highly elastic materials, i.e. for materials in which energy is conserved in a cycle of deformation carried out under isothermal conditions. Now, it is well known that rubber vulcanizates exhibit in greater or lesser degree the effects of hysteresis, internal friction and permanent set. These effects represent departures from the ideal elasticity envisaged by the theory, and it is therefore important to design the experiments in such a manner that the influence of these departures is minimized.

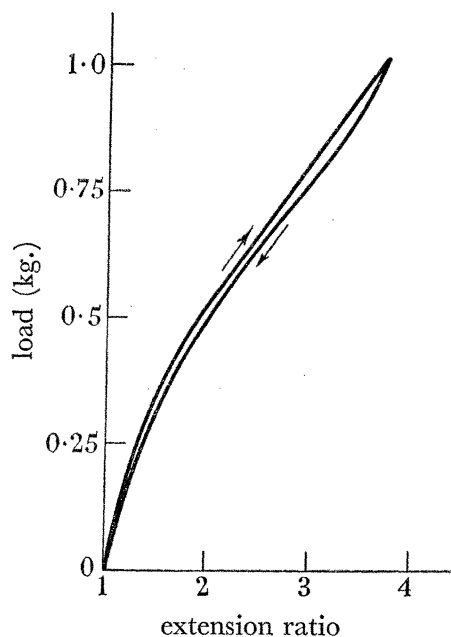


FIGURE 1. Typical load-extension ratio curve for rubber in simple extension.  
(Initial cross-section = 0.108 cm.<sup>2</sup>.)

In order to minimize the effects of hysteresis, a pure gum mix of natural rubber, without added fillers or reinforcing agents, was used in making the test-pieces. It is seen from figure 1, in which are shown the load-extension ratio curves for a test-piece of the rubber, obtained under conditions of increasing load and decreasing load, that the hysteresis is very small. In the interests of consistency, in all the experiments the load-increasing direction has been used in obtaining the load-deformation curves.

If a natural rubber vulcanizate, such as is used in the experiments, is subjected at normal room temperature to a sufficiently large deformation, it is well known that crystallization occurs. This crystallization disappears when the load is removed. However, in the region of deformation for which it occurs, it is accompanied by abnormally high hysteresis, the load-deformation relations being to a high degree irreversible. In order to avoid difficulties arising from this effect, the experiments—or, at any rate, their interpretation in terms of the theory—were confined to deformations for which crystallization does not occur. It should, however, be remarked that it is at present not clear exactly to what extent the presence of crystallization would be expected to invalidate the application of the theory.



Test-pieces made from a well-vulcanized pure gum mix also show extremely small permanent set unless they are left in the deformed state for a very long time or are subjected to too extensive a cycle of deformations. In order to minimize the effects of permanent set and any anisotropy arising from it on the experimental results, the same test-piece was not used for too many experiments.

The necessity for taking account of internal friction was avoided by restricting the experiments to static conditions of loading.

In each of the experiments described in this paper one of two recipes was used in preparing the vulcanized rubber test-pieces. These are referred to as *A* and *B* and are given in §20. In principle, it would have been preferable to use a single recipe for all of the test-pieces. In view of the general similarity in the behaviour of the rubbers prepared according to the two recipes and the fact that even if a single recipe were used we should not be able to count on the various test-pieces being identical in their properties, it was considered that no purpose, except perhaps the aesthetic, would be served by repeating any extensive series of experiments.

## A. EXPERIMENTS ON PURE HOMOGENEOUS DEFORMATION

### 2. THEORETICAL CONSIDERATIONS

If the stored-energy function  $W$  for an ideal incompressible highly elastic material which is isotropic in its undeformed state is known in terms of the invariants of strain  $I_1$  and  $I_2$ , then it can be shown (Rivlin 1948 *d*) that the principal components of stress  $t_i$  ( $i = 1, 2, 3$ ) associated with the pure homogeneous deformation of the material, for which the extension ratios are  $\lambda_i$  ( $i = 1, 2, 3$ ), are given by

$$t_i = 2 \left[ \lambda_i^2 \frac{\partial W}{\partial I_1} - \frac{1}{\lambda_i^2} \frac{\partial W}{\partial I_2} \right] + p \quad (i = 1, 2, 3), \quad (2.1)$$

where  $p$  is an arbitrary hydrostatic pressure.

Now consider a thin plane rectangular sheet of the material of uniform thickness, having its major surfaces normal to the  $z$ -axis and its edges parallel to the  $x$ - and  $y$ -axes of a rectangular Cartesian co-ordinate system  $(x, y, z)$ . If this is deformed in a pure homogeneous manner so that the principal directions of the strain are parallel to  $x$ ,  $y$  and  $z$  and the extension ratios in these directions are  $\lambda_1$ ,  $\lambda_2$  and  $\lambda_3$  respectively, we see that  $t_3 = 0$  (since the major surfaces are force-free) and employing the relation  $\lambda_1 \lambda_2 \lambda_3 = 1$ , expressing the incompressibility of the material, equations (2.1) yield

$$\left. \begin{aligned} t_1 &= 2 \left( \lambda_1^2 - \frac{1}{\lambda_1^2 \lambda_2^2} \right) \left( \frac{\partial W}{\partial I_1} + \lambda_2^2 \frac{\partial W}{\partial I_2} \right) \\ t_2 &= 2 \left( \lambda_2^2 - \frac{1}{\lambda_1^2 \lambda_2^2} \right) \left( \frac{\partial W}{\partial I_1} + \lambda_1^2 \frac{\partial W}{\partial I_2} \right) \end{aligned} \right\} \quad (2.2)$$

and

The forces  $f_1$  and  $f_2$  per unit length of edge measured in the undeformed state are given by

$$f_1 = t_1 h / \lambda_1 \quad \text{and} \quad f_2 = t_2 h / \lambda_2, \quad (2.3)$$

where  $h$  is the thickness of the sheet in its undeformed state.

Measurements of  $f_1$  and  $f_2$  for any values of  $\lambda_1$  and  $\lambda_2$  enable us to calculate  $t_1$  and  $t_2$  from equations (2.3) and, from these, the corresponding values of  $\partial W/\partial I_1$  and  $\partial W/\partial I_2$  can be found by solving equations (2.2) as

$$\left. \begin{aligned} \frac{\partial W}{\partial I_1} &= \frac{\lambda_1^2 t_1}{\lambda_1^2 - 1/\lambda_1^2 \lambda_2^2} - \frac{\lambda_2^2 t_2}{\lambda_2^2 - 1/\lambda_1^2 \lambda_2^2} \\ \frac{\partial W}{\partial I_2} &= \frac{t_1}{\lambda_1^2 - 1/\lambda_1^2 \lambda_2^2} - \frac{t_2}{\lambda_2^2 - 1/\lambda_1^2 \lambda_2^2} \end{aligned} \right\} \quad (2.4)$$

and

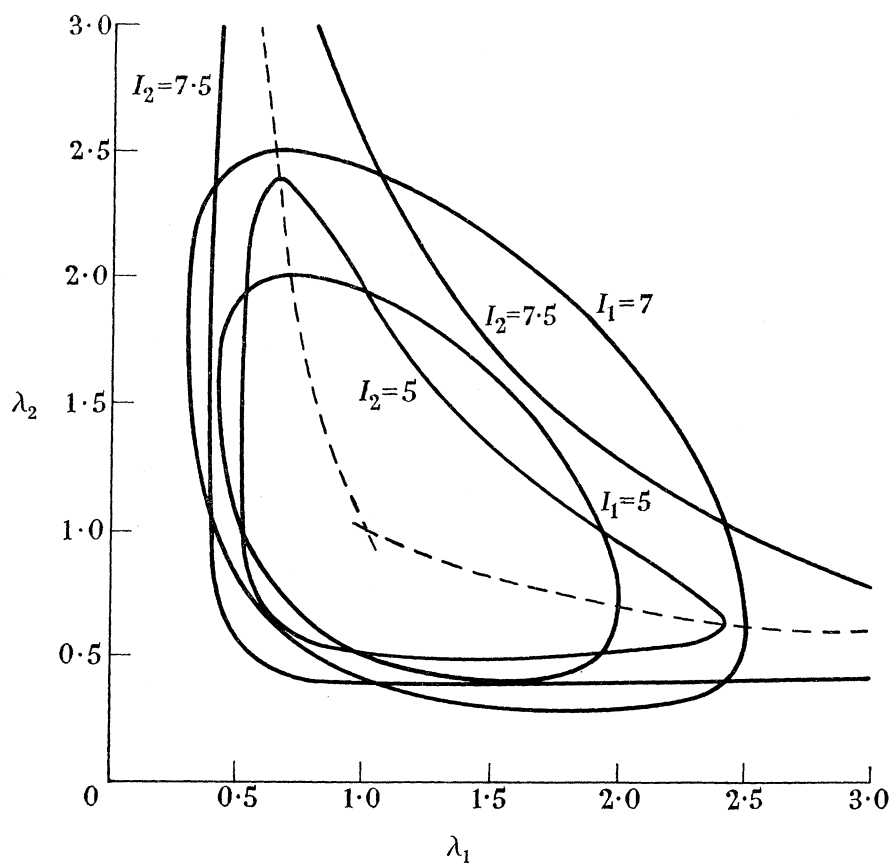


FIGURE 2. The relation between  $\lambda_1$  and  $\lambda_2$  at constant  $I_1$  or  $I_2$ .

The values of  $I_1$  and  $I_2$  for which equations (2.4) express the values of  $\partial W/\partial I_1$  and  $\partial W/\partial I_2$  are, of course, given in terms of  $\lambda_1$  and  $\lambda_2$  by

$$I_1 = \lambda_1^2 + \lambda_2^2 + \frac{1}{\lambda_1^2 \lambda_2^2} \quad \text{and} \quad I_2 = \frac{1}{\lambda_1^2} + \frac{1}{\lambda_2^2} + \lambda_1^2 \lambda_2^2. \quad (2.5)$$

If as  $\lambda_1$  is varied,  $\lambda_2$  is varied in such a manner that  $I_2$  remains constant, we obtain values of  $\partial W/\partial I_1$  and  $\partial W/\partial I_2$  for various values of  $I_1$  at constant  $I_2$ . Similarly, if  $\lambda_1$  and  $\lambda_2$  are varied in such a manner that  $I_1$  remains constant, we obtain the values of  $\partial W/\partial I_1$  and  $\partial W/\partial I_2$  for various values of  $I_2$  at constant  $I_1$ . In this way a set of curves can be obtained for the material showing how  $\partial W/\partial I_1$  and  $\partial W/\partial I_2$  depend on  $I_1$  and  $I_2$ .

Corresponding values of  $\lambda_1$  and  $\lambda_2$  for which  $I_1$  is constant are given, from the first of equations (2.5), by the relation

$$\lambda_2^2 = \frac{1}{2}\{(I_1 - \lambda_1^2) \pm [(I_1 - \lambda_1^2)^2 - 4/\lambda_1^2]^{\frac{1}{2}}\}. \quad (2.6)$$

Corresponding values of  $\lambda_1$  and  $\lambda_2$  for which  $I_2$  is constant are given, from the second of equations (2.5), by the relation

$$\lambda_2^2 = \frac{1}{2\lambda_1^2} \left\{ \left( I_2 - \frac{1}{\lambda_1^2} \right) \pm \left[ \left( I_2 - \frac{1}{\lambda_1^2} \right)^2 - 4\lambda_1^2 \right]^{\frac{1}{2}} \right\}. \quad (2.7)$$

The manner in which  $\lambda_1$  and  $\lambda_2$  vary for certain constant values of  $I_1$  and  $I_2$  is shown in figure 2.

For simple extension parallel to the  $x$ -axis, we have

$$\lambda_2 = \lambda_1^{-\frac{1}{2}}, \quad (2.8)$$

and for simple extension parallel to the  $y$ -axis, we have

$$\lambda_1 = \lambda_2^{-\frac{1}{2}}. \quad (2.9)$$

These correspond to the experimental situations in which  $f_1$  and  $f_2$  are respectively made zero. The relations (2.8) and (2.9) are plotted as the broken curves in figure 2.

### 3. THE EXPERIMENTAL ARRANGEMENT

It can be seen from the theoretical considerations of the previous section that if the forces which must be applied to the edges of a thin rectangular rubber sheet in order to produce a pure homogeneous deformation in it are measured for various values of the extension ratios  $\lambda_1$  and  $\lambda_2$ , chosen in such a way that either  $I_1$  or  $I_2$  is constant, we can in principle, by choosing a number of values for this constant, find how  $\partial W/\partial I_1$  and  $\partial W/\partial I_2$  depend on  $I_1$  and  $I_2$ .

The experiments were carried out using a square test-piece of vulcanized natural rubber *A* (see §20 for formulation) having 8 cm. sides, cut from a sheet about 0.7 mm. thick. The test-piece was cut so that five lugs were formed on each of its sides and the surface of the sheet was marked in ink with two sets of four parallel straight lines forming a 3 cm. square grid of 1 cm. spacing.

In order to produce the deformation, strings were tied to the lugs, and by means of these the test-piece was supported in a large square frame constructed of brass curtain rail and mounted horizontally, as shown in figure 3. Each of the twenty strings carried at its other end a small tent runner, by means of which its effective length could be adjusted, and passed through a small ring attached to a roller which could run freely on the brass rails. By altering the effective lengths of the strings, tensions could be applied to the rubber sheet and, by adjusting appropriately the positions on the rails of the brass rollers, the directions of the strings and therefore of the tensions applied to the sheet could be maintained in two perpendicular directions. Small calibrated helical springs were attached between the rings and the rollers on the three central strings on each of two adjacent sides of the test-piece. These were used to measure the tensions in the strings.

In the experiments, forces were applied to the test-piece by adjusting the lengths of the strings by means of the runners, in such a manner that the nine squares of the grid were



deformed into rectangles of identical dimensions, so that this portion of the test-piece was substantially in a state of pure homogeneous strain. The ratios of the lengths of the sides of the rectangles in their deformed and undeformed states gave the values of the principal extension ratios  $\lambda_1$  and  $\lambda_2$  for the deformation. It was assumed that the forces operative in producing the pure homogeneous deformation of the central nine squares were those applied by the central three strings on each side of the test-piece, and the forces  $f_1$  and  $f_2$ , defined in §2, were taken as the means of the tensions measured in the central three strings on the appropriate sides of the test-piece. This is justified by the preliminary experiments discussed in appendix 3 (§22).

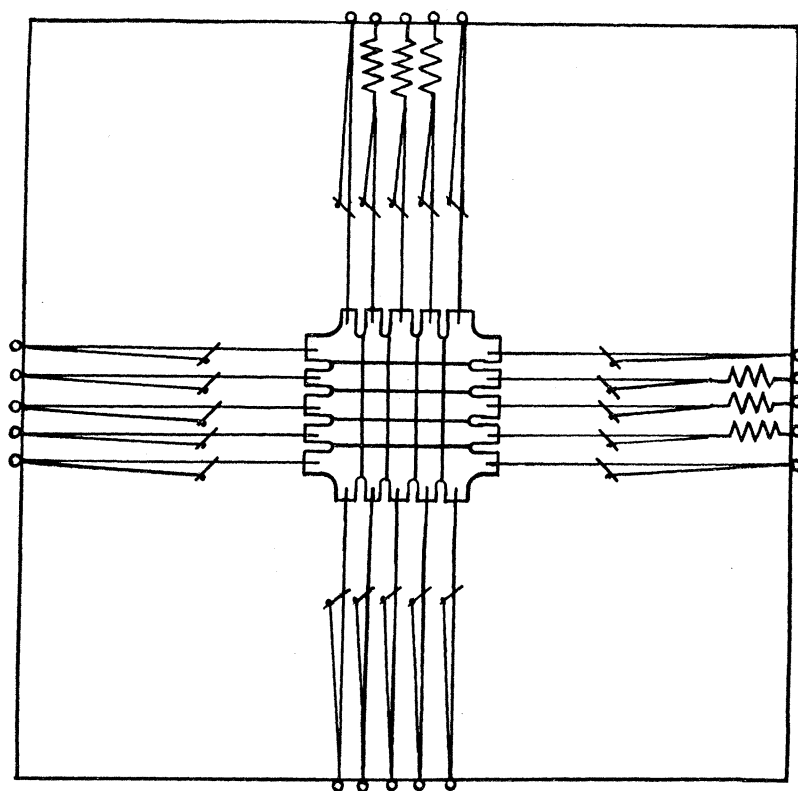


FIGURE 3. Experimental arrangement for experiment on pure homogeneous deformation with  $I_1$  or  $I_2$  constant.

The method described above for measuring the forces necessary to produce a pure homogeneous strain in a rubber sheet is a modification of that employed by Treloar (1948). It has the advantage, from the point of view of the present experiments, of allowing greater simplicity in the adjustment of the strains to their desired values.

In the present experiments the extension ratios  $\lambda_1$  and  $\lambda_2$  were varied together so that  $I_1$  had a constant chosen value. The procedure was then repeated for various values of  $I_1$ . Then,  $\lambda_1$  and  $\lambda_2$  were varied together so that  $I_2$  had a constant chosen value and the procedure was repeated for various values of  $I_2$ . In varying  $\lambda_1$  and  $\lambda_2$ , it was always arranged that  $\lambda_1$  should decrease steadily while  $\lambda_2$  increased steadily. For any value of  $\lambda_1$  and of  $I_1$  or  $I_2$  the corresponding value of  $\lambda_2$  was determined from graphs of the type shown in figure 2, but plotted on a larger scale. It may be noted that with the experimental arrangement described above,

the forces  $f_1$  and  $f_2$  applied to the rubber must always be tensile or zero. As a result, the only experimentally realizable pairs of values of  $\lambda_1$  and  $\lambda_2$  are those which lie to the right and above the broken lines in figure 2 representing simple extension.

#### 4. EXPERIMENTAL RESULTS

The values of  $t_1$  and  $t_2$  corresponding to specified values of  $\lambda_1$  and  $\lambda_2$  are calculated by (2.3) from the values of  $f_1$  and  $f_2$  obtained in the manner described in §3, using the measured value of  $h$ . In table 1, these values of  $t_1$  and  $t_2$  are given, for various values, of  $\lambda_1$  and  $\lambda_2$  related in such a way that  $I_1 = 5, 7, 9$  and  $11$ . In table 2 their values are given for various values of  $\lambda_1$  and  $\lambda_2$  related in such a way that  $I_2 = 5, 10, 20$  and  $30$ .

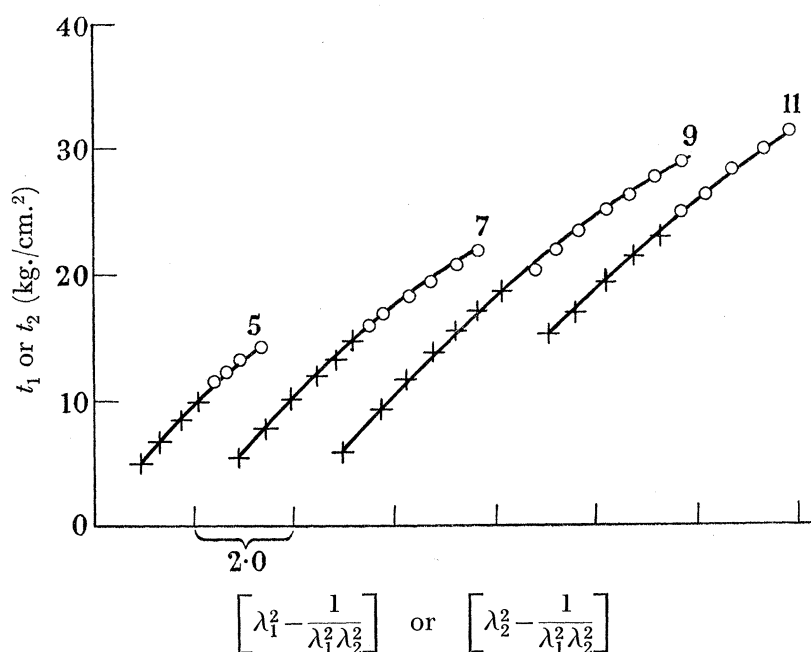


FIGURE 4. Plot of  $t_1$  and  $t_2$  against  $(\lambda_1^2 - 1/\lambda_1^2 \lambda_2^2)$  and  $(\lambda_2^2 - 1/\lambda_1^2 \lambda_2^2)$  respectively at constant  $I_1$ . (The crosses denote  $t_2$  and the circles  $t_1$ ; the origin is shifted by two units parallel to the abscissa for each increment in the value of  $I_1$ .)

In figure 4, the values of  $t_1$  and  $t_2$  given in table 1 are plotted against  $(\lambda_1^2 - 1/\lambda_1^2 \lambda_2^2)$  and  $(\lambda_2^2 - 1/\lambda_1^2 \lambda_2^2)$  respectively at constant  $I_1$ . For each increment in the value of  $I_1$  for which the results are plotted, the origin for the appropriate curve is shifted parallel to the abscissa by two units.

It is seen from the first row of table 1 that when  $\lambda_1 = 1.90$  and  $\lambda_2 = 1.07$ , we obtain values for  $t_1$  and  $t_2$  of  $13.9$  and  $4.9$  kg./cm.<sup>2</sup> respectively. Now, provided that the material is isotropic in its undeformed state, we can see that an interchange in the values of  $\lambda_1$  and  $\lambda_2$  should lead to an interchange in the measured values of  $t_1$  and  $t_2$ , i.e. for  $\lambda_1 = 1.07$  and  $\lambda_2 = 1.90$  we obtain values of  $t_1$  and  $t_2$  of  $4.9$  and  $13.9$  kg./cm.<sup>2</sup> respectively. This argument applies to the results given in each row of the table so that each row yields two points in figure 4.

TABLE 1

$I_1$	$\lambda_1$	$\lambda_2$	$t_1$ (kg./cm. <sup>2</sup> )	$t_2$ (kg./cm. <sup>2</sup> )	$I_2$	$\partial W/\partial I_1$ (kg./cm. <sup>2</sup> )	$\partial W/\partial I_2$ (kg./cm. <sup>2</sup> )
5	1.90	1.07	13.9	4.9	5.28	1.77	0.20
	1.80	1.25	12.8	6.3	6.01	1.89	0.23
	1.70	1.39	12.0	8.1	6.45	2.01	0.21
	1.60	1.51	10.9	9.6	6.67	—	—
7	2.40	1.04	21.6	5.2	7.33	1.72	0.19
	2.30	1.25	20.2	7.7	9.10	1.66	0.19
	2.20	1.43	19.2	9.8	10.59	1.66	0.18
	2.10	1.58	17.9	11.8	11.63	1.58	0.20
	2.00	1.71	16.7	13.2	12.27	1.60	0.18
9	1.90	1.82	15.6	14.5	12.54	—	—
	2.80	1.02	29.1	5.7	9.24	1.70	0.18
	2.70	1.28	27.7	9.0	12.69	1.64	0.17
	2.60	1.47	26.3	11.3	15.22	1.61	0.16
	2.50	1.64	24.9	13.6	17.34	1.59	0.16
	2.40	1.80	23.0	15.3	19.14	1.53	0.15
	2.30	1.91	21.5	16.5	19.76	1.49	0.15
11	2.20	2.03	20.2	18.4	20.40	—	—
	2.80	1.76	31.5	15.1	24.74	1.73	0.09
	2.70	1.91	29.9	17.2	27.01	1.79	0.07
	2.60	2.05	28.3	19.1	28.79	1.80	0.07
	2.50	2.18	26.7	21.1	30.07	1.85	0.06
	2.40	2.28	25.0	22.8	30.31	—	—

TABLE 2

$I_2$	$\lambda_1$	$\lambda_2$	$t_1$ (kg./cm. <sup>2</sup> )	$t_2$ (kg./cm. <sup>2</sup> )	$I_1$	$\partial W/\partial I_1$ (kg./cm. <sup>2</sup> )	$\partial W/\partial I_2$ (kg./cm. <sup>2</sup> )
5	2.40	0.69	20.1	0.56	6.60	—	—
	2.30	0.76	18.3	1.87	6.20	—	—
	2.20	0.83	16.7	2.27	5.92	1.66	0.26
	2.10	0.89	15.5	2.94	5.49	1.65	0.28
	2.00	0.96	14.8	3.47	5.19	1.78	0.22
	1.90	1.02	13.2	4.22	4.92	1.68	0.29
	1.80	1.09	12.0	4.52	4.69	1.76	0.21
	1.70	1.17	10.8	4.8 (5)	4.51	—	—
	1.60	1.24	9.8	6.0 (5)	4.35	—	—
	1.50	1.33	8.4	6.9	4.27	—	—
	10	2.80	1.07	27.9	6.1	9.10	1.61
2.70		1.11	26.2	6.5	8.63	1.61	0.18
2.60		1.16	24.6	7.0	8.13	1.63	0.18
2.50		1.21	22.9	7.4	7.82	1.61	0.18
2.40		1.26	21.3	7.9	7.46	1.59	0.19
2.30		1.32	19.8	8.6	7.14	1.56	0.20
2.20		1.38	18.3	9.0	6.85	1.57	0.19
2.10		1.45	17.0	9.7	6.62	1.52	0.22
2.00		1.53	15.9	10.4	6.45	—	—
1.90		1.61	14.7	11.2	6.31	—	—
1.80		1.70	13.5	12.1	6.24	—	—
20	2.80	1.58	30.4	12.4	10.39	1.67	0.11
	2.70	1.63	28.5	12.9	10.00	1.68	0.11
	2.60	1.70	26.7	13.6	9.80	1.69	0.10
	2.50	1.76	24.8	14.2	9.40	1.68	0.11
	2.40	1.84	23.1	15.0	9.20	1.69	0.10
	2.30	1.92	21.6	16.0	9.03	—	—
	2.20	2.01	20.1	17.0	8.95	—	—
30	2.80	1.94	31.8	18.0	11.64	1.69	0.09
	2.70	2.02	29.8	18.8	11.40	1.71	0.08
	2.60	2.09	27.8	19.6	11.16	1.72	0.08
	2.50	2.18	26.3	20.8	11.04	—	—
	2.40	2.27	24.2	21.9	10.95	—	—

In figure 5, the values of  $t_1$  and  $t_2$  given in table 2 are plotted against  $(\lambda_1^2 - 1/\lambda_1^2\lambda_2^2)$  and  $(\lambda_2^2 - 1/\lambda_1^2\lambda_2^2)$  respectively at constant  $I_2$  in a similar manner. There again each row of the table gives two points in the figure.

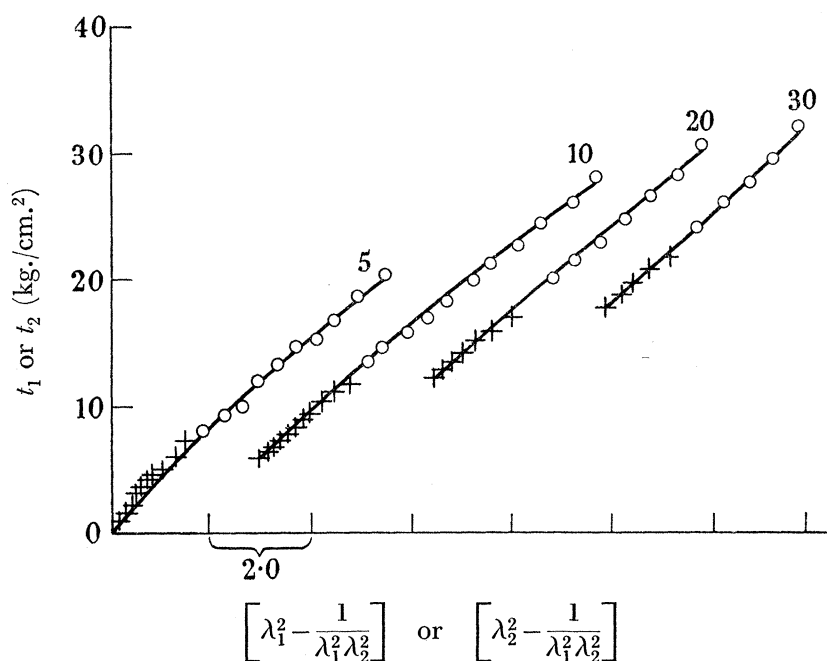


FIGURE 5. Plot of  $t_1$  and  $t_2$  against  $(\lambda_1^2 - 1/\lambda_1^2\lambda_2^2)$  and  $(\lambda_2^2 - 1/\lambda_1^2\lambda_2^2)$  respectively at constant  $I_2$ . (The crosses denote  $t_2$  and the circles  $t_1$ ; the origin is shifted by two units parallel to the abscissa for each increment in the value of  $I_2$ .)

For each value of  $\lambda_1$  and  $\lambda_2$  given in tables 1 and 2, the corresponding values of  $\partial W/\partial I_1$  and  $\partial W/\partial I_2$  can be calculated by equations (2.4), and the values found are given in the seventh and eighth columns of the tables. In calculating  $\partial W/\partial I_1$  and  $\partial W/\partial I_2$  it is seen from (2.4) that any error in  $t_1$  or  $t_2$  is reflected in a greater percentage error in the calculated values of  $\partial W/\partial I_1$  and  $\partial W/\partial I_2$ , particularly in the latter. This magnification of the experimental error becomes more and more pronounced as  $\lambda_1$  and  $\lambda_2$  tend to equality. In the limiting case, when  $\lambda_1 = \lambda_2$ ,  $t_1$  should be equal to  $t_2$ , and the values given by equations (2.4) for  $\partial W/\partial I_1$  and  $\partial W/\partial I_2$  are indeterminate. Consequently, the calculated values of  $\partial W/\partial I_1$  and  $\partial W/\partial I_2$  for values of  $\lambda_1$  and  $\lambda_2$  which are very nearly equal are not given in tables 1 and 2, as being too inaccurate to have any significance.

Also, the probable errors in the values of  $t_1$  and  $t_2$  given in tables 1 and 2 are likely to be more nearly absolute in value than proportional to the magnitudes of  $t_1$  and  $t_2$ . Consequently, the lower values of  $t_1$  and  $t_2$  are likely to be subject to the greatest percentage errors. It is seen that the worst situation in this respect occurs in the first rows of table 2, where  $t_2$  has very low values. The percentage error thus introduced into  $\partial W/\partial I_2$  is much greater than that introduced into  $\partial W/\partial I_1$  and is sufficiently great to make the values of  $\partial W/\partial I_2$  in the first two rows of table 2 too unreliable to be of value.

It can be seen from tables 1 and 2, that, for the values of  $I_1$  and  $I_2$  in the range covered by the experiments,  $\partial W/\partial I_1$  does not appear to vary significantly with  $I_1$  and  $I_2$  and  $\partial W/\partial I_2$  does not appear to vary significantly with  $I_1$ , but decreases as  $I_2$  increases. For the lower

values of  $I_2$ ,  $(\partial W/\partial I_2)/(\partial W/\partial I_1)$  is about  $\frac{1}{3}$  and decreases with increase in  $I_2$ . This is shown more clearly in figure 6, where  $\partial W/\partial I_1$  and  $\partial W/\partial I_2$  are plotted against  $I_1$  and  $I_2$ . In view of the relatively large experimental errors involved, it cannot, however, be asserted that  $\partial W/\partial I_1$  is

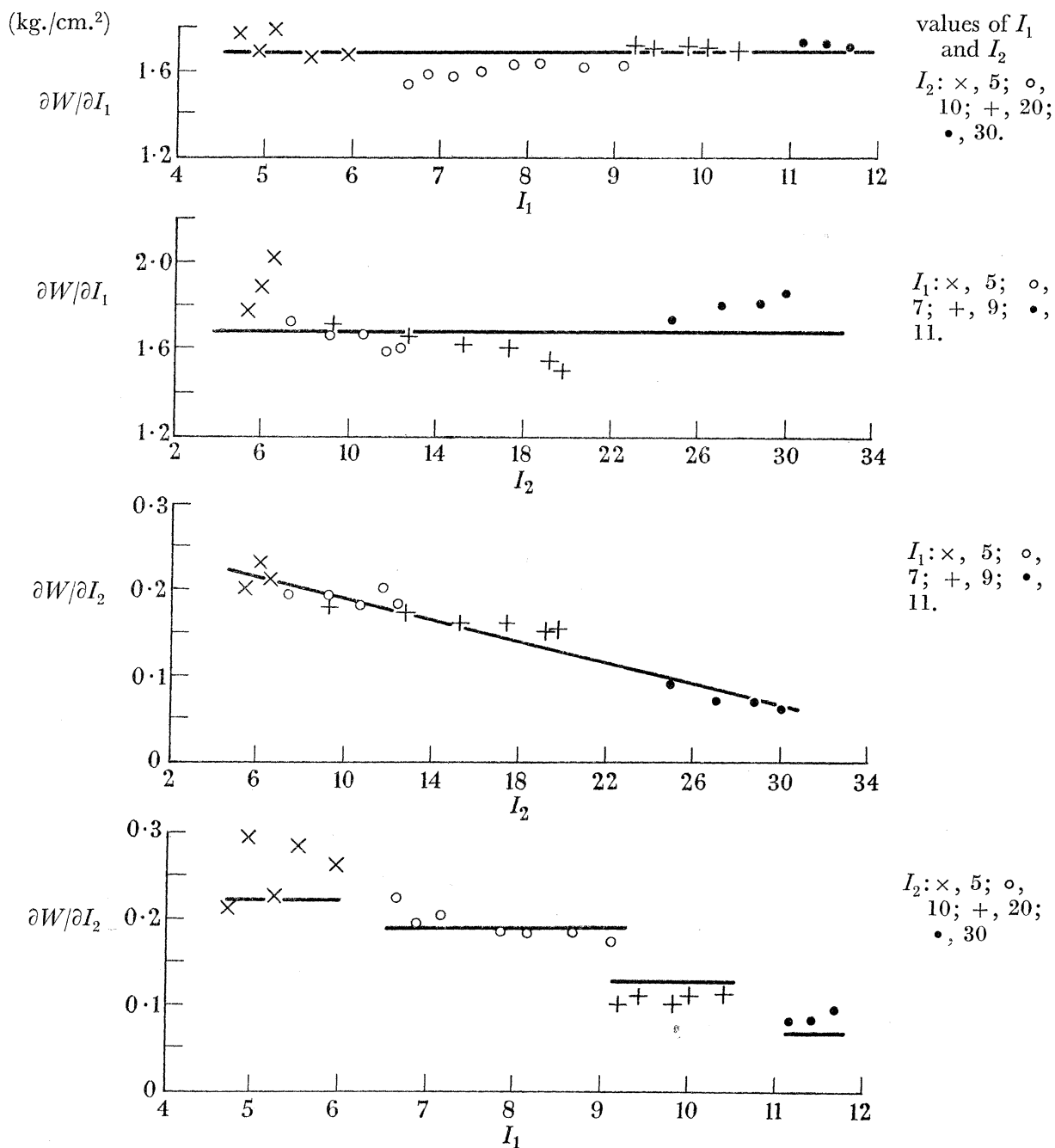


FIGURE 6. Plot of  $\partial W/\partial I_1$  and  $\partial W/\partial I_2$  against  $I_1$  and  $I_2$ .

absolutely constant, or that  $\partial W/\partial I_2$  is absolutely independent of  $I_1$ . If, however, the full lines in figure 6 are taken as representing the true dependence of  $\partial W/\partial I_1$  and  $\partial W/\partial I_2$  on  $I_1$  and  $I_2$  and, from the values so given, the dependence of the stress components  $t_1$  and  $t_2$  on  $I_2$ , with  $I_1$  constant, and on  $I_1$ , with  $I_2$  constant, can be calculated. The full lines in figures 4 and 5 are obtained. It is seen that they represent very accurately the experimental results. It is,



however, possible that the experimental results could be equally well represented by some slightly different dependence of  $\partial W/\partial I_1$  and  $\partial W/\partial I_2$  on  $I_1$  and  $I_2$ . If this were the case, however, it would not, from the practical point of view of predicting the behaviour of a rubber object under load, significantly affect the predictions of the theory, and consequently we might just as well use the type of dependence chosen.\*

### 5. EXPERIMENTS AT LOW VALUES OF $I_1$ AND $I_2$

It has been seen in § 4 that the experimental errors involved in the experiments on the pure homogeneous deformation of a rubber sheet described in § 3 become proportionately greater as the measured values of  $f_1$  and  $f_2$ —and hence of the stress components  $t_1$  and  $t_2$ —decrease. Since, in general,  $t_1$  and  $t_2$  decrease with  $I_1$  and  $I_2$ , this sets a lower limit on the values of  $I_1$  and  $I_2$  for which the method described can be used to determine  $\partial W/\partial I_1$  and  $\partial W/\partial I_2$ . In practice it was not found convenient to use the method for values of  $I_1$  and  $I_2$  less than about 5.

For lower values of  $I_1$  and  $I_2$  than this, some indication of the manner in which  $\partial W/\partial I_1$  and  $\partial W/\partial I_2$  vary with  $I_1$  and  $I_2$  can be obtained by carrying out experiments in which a rectangular sheet of rubber is subjected to a pure homogeneous deformation, of principal extension ratios  $\lambda_1$  and  $\lambda_2$ , for which, instead of maintaining  $I_1$  and  $I_2$  constant at various values as the deformation is varied,  $\lambda_2$  is maintained constant and the dependence of  $\lambda_1$  on the applied load in the direction of  $\lambda_1$  is measured.

It is seen from equations (2.2) that the stress  $t_1$  in the direction of the extension ratio  $\lambda_1$  is given by

$$t_1 = 2\left(\lambda_1^2 - \frac{1}{\lambda_1^3 \lambda_2^2}\right) \left(\frac{\partial W}{\partial I_1} + \lambda_2^2 \frac{\partial W}{\partial I_2}\right), \quad (5.1)$$

where  $I_1$  and  $I_2$  are given by (2.5). If the cross-sectional area of the sheet normal to the direction of  $\lambda_1$  is  $A$ , in the undeformed state, then the load  $N$  is given by

$$N = 2A\left(\lambda_1 - \frac{1}{\lambda_1^3 \lambda_2^2}\right) \left(\frac{\partial W}{\partial I_1} + \lambda_2^2 \frac{\partial W}{\partial I_2}\right). \quad (5.2)$$

In § 6 an experiment is described in which a rectangular sheet of rubber was subjected to pure shears of various magnitudes and the corresponding load was measured. This involved loading the test-piece in such a way that  $\lambda_1$  could be varied while  $\lambda_2 = 1$ .

In § 7 an experiment is described in which a rectangular sheet of rubber was subjected simultaneously to a constant simple extension and a pure shear of variable magnitude. This involved loading the test-piece in such a way that  $\lambda_1$  could be varied while  $\lambda_2$  was maintained at a constant value less than unity.

In § 9 an experiment on the simple extension of a rubber strip is described. For simple extension  $\lambda_2 = \lambda_1^{-1}$ , so that, writing  $\lambda$  for  $\lambda_1$ , equation (5.2) yields

$$N = 2A\left(\lambda - \frac{1}{\lambda^2}\right) \left(\frac{\partial W}{\partial I_1} + \frac{1}{\lambda} \frac{\partial W}{\partial I_2}\right), \quad (5.3)$$

and equations (2.5) yield  $I_1 = \lambda^2 + \frac{2}{\lambda}$  and  $I_2 = 2\lambda + \frac{1}{\lambda^2}$ . (5.4)

\* This statement is not always entirely correct, but it would be an over-elaboration to enter into the qualifications at this stage.

In order to make the results of these experiments directly comparable, the test-pieces were all cut from a single sheet of vulcanized rubber  $A$  (see §20 for formulation). This had a thickness of 0.87 mm., and from it the three rectangular test-pieces were cut with approximate dimensions (in cm.)  $9.5 \times 2$ ,  $9.5 \times 15$  and  $0.8 \times 5$ . The first of these was used for the experiments on pure shear, the second for the experiments in which a constant simple extension was superposed on the pure shear and the last for the experiments on simple extension.

#### 6. EXPERIMENT ON PURE SHEAR

The test-piece was marked in ink with two fine lines  $AA'$  and  $BB'$ , as shown in figure 7. It was held firmly in two wide metal clamps  $C_1$  and  $C_2$  very close and parallel to the lines  $AA'$  and  $BB'$ .

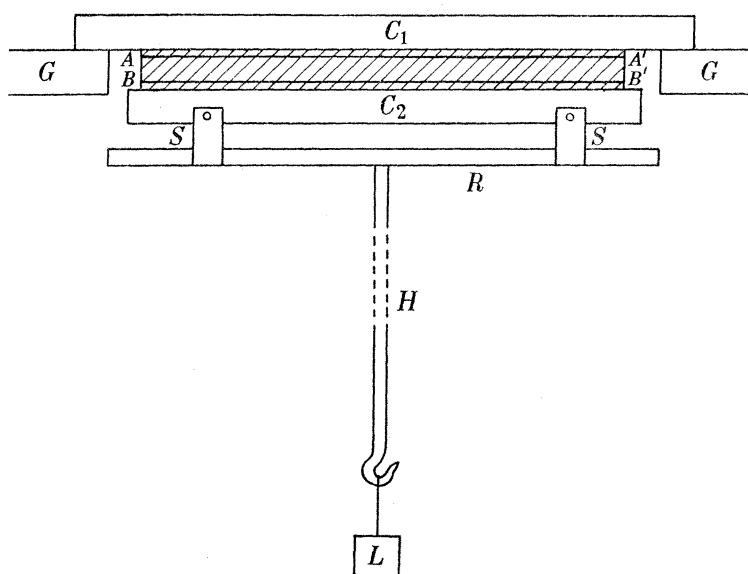


FIGURE 7. Experimental arrangement for experiment on pure shear.

Ideally, in order to produce a pure shear in the region  $AA'B'B$ , it is necessary to increase the separation between  $AA'$  and  $BB'$  while maintaining the rectangular form of the region  $AA'B'B$  and leaving the lengths of the edges  $AA'$  and  $BB'$  unchanged. When the clamps are separated in a direction parallel to  $AB$  by loading, the rectangular form of the region  $AA'B'B$  is not accurately preserved, a contraction of the central region taking place in a direction parallel to  $AA'$  and  $BB'$ . In a preliminary experiment, in which the distance between  $AA'$  and  $BB'$  was extended to 2.2 times its length in the undeformed state of the sheet, it was found that the lengths of  $AA'$  and  $BB'$  did not change appreciably, while the length of a line midway between and parallel to  $AA'$  and  $BB'$  decreased by only 3%. It will be seen that this change is not likely to have a significant effect on the results and can therefore be neglected.

In performing the experiment, the clamp  $C_1$ , which was larger than the clamp  $C_2$ , was supported horizontally on two rigid supports  $G$ , as shown in figure 7. The lower clamp  $C_2$  carried stirrups  $S$  in which a rod  $R$  could be moved in a horizontal direction. The long rod  $H$ , carrying a hook to which the load was attached, was rigidly attached to  $R$  at right angles

to it. With this arrangement it was found possible, by suitably adjusting the position of  $R$  in the stirrups  $S$ , to ensure that when the load was varied the clamp  $C_2$  did not tilt so that the line  $BB'$  was maintained accurately horizontal and in the same vertical plane as  $AA'$ .

#### 7. EXPERIMENT ON PURE SHEAR SUPERPOSED ON SIMPLE EXTENSION

The test-piece  $PQQ'P'$  was marked in ink with six lines as shown in figure 8. In the undeformed state of the rubber, the distance between  $BB'$  and  $CC'$  was 0.4 cm. The test-piece was first held firmly in two clamps with their edges along  $AA'$  and  $DD'$  and stretched, by separating the clamps, until the lengths of  $BB'$  and  $CC'$  were reduced to about three-quarters of their initial value.

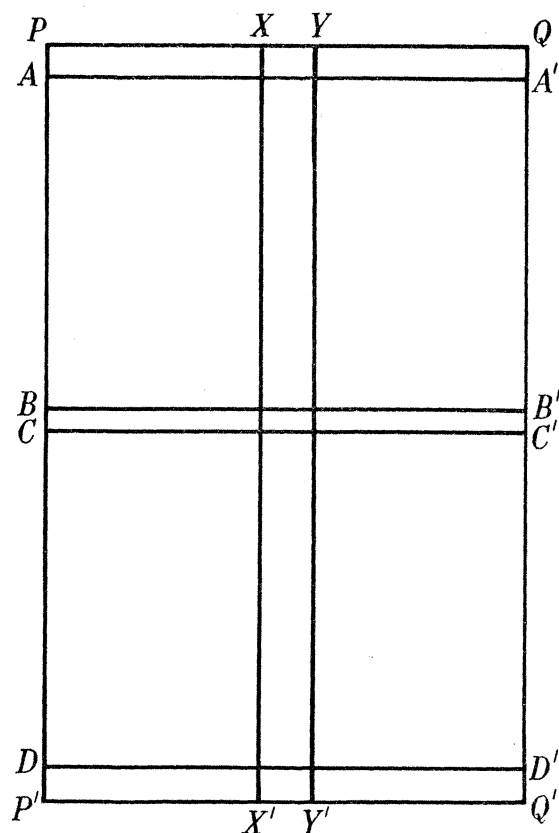


FIGURE 8. Test-piece for experiment on pure shear superposed on simple extension.

While the rubber sheet was held in this state of deformation, two further clamps were employed to clamp the sheet firmly along  $BB'$  and  $CC'$ . The clamps at  $AA'$  and  $DD'$  were then removed.

The experiment was performed in a manner similar to that adopted in the experiment on pure shear described in § 6 and illustrated in figure 7. The distances between the lines  $BB'$  and  $CC'$  were found for various states of loading of the specimen and their ratios to this distance measured in the undeformed state of the rubber gave the values of  $\lambda_1$ , the extension ratio in the direction of the applied load, corresponding to the various values of the load. The extension ratio  $\lambda_2$  in the plane of the sheet and at right angles to the direction of the applied load was found to be constant to about  $\frac{1}{2}$  % over the whole range of loads employed,

by measuring the distances in the deformed states between  $XX'$  and  $YY'$  with a travelling microscope. From the ratio of this distance to the corresponding distance measured in the undeformed state, the value obtained for  $\lambda_2$  was  $0.776 \pm 0.008$ .

Owing to the initial extension of the rubber sheet, it buckled when no load was applied and consequently measurements were made only at greater values of the load than about 4 kg., at which value this buckling disappeared.

## 8. EXPERIMENTAL RESULTS

In table 3 are given the results of the experiment on pure shear described in §6. In the first and second columns, corresponding values of the load  $N$  and extension ratio  $\lambda_1$  in the direction of the load are given. From equation (5.2), bearing in mind that  $\lambda_2 = 1$ , we can then calculate  $(\partial W/\partial I_1 + \partial W/\partial I_2)$  for each value of  $\lambda_1$ , and the values so obtained are given in the third column of the table. In the remaining column corresponding values of  $I_1$  and  $I_2$  are given.

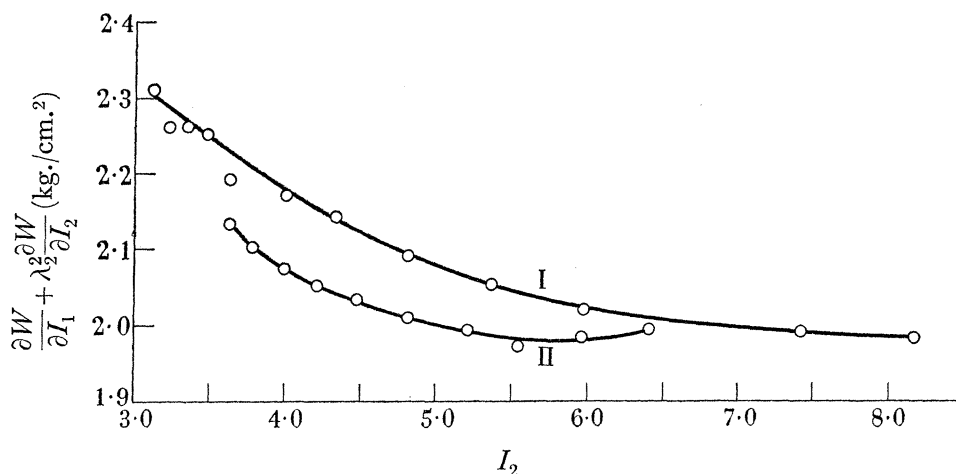


FIGURE 9. Plot of  $(\partial W/\partial I_1 + \lambda_2^2 \partial W/\partial I_2)$  against  $I_2$  from experiments on pure shear and pure shear superposed on simple extension. Curve I, pure shear ( $\lambda_2 = 1$ ); curve II, pure shear superposed on simple extension ( $\lambda_2 = 0.776$ ).

In table 4 are given the results obtained in the experiment on superposed elongation and pure shear described in §7. Again, in the first and second columns, corresponding values of the load  $N$  and extension ratio  $\lambda_1$  in the direction of the load are given. From equation (5.2), the value of  $(\partial W/\partial I_1 + \lambda_2^2 \partial W/\partial I_2)$  is calculated for each value of  $\lambda_1$ , employing the constant value of  $\lambda_2 = 0.776$ . In the remaining columns, the corresponding values of  $I_1$  and  $I_2$  are given.

If we assume that  $\partial W/\partial I_1$  and  $\partial W/\partial I_2$  are independent of  $I_1$  and depend on  $I_2$  only, we can plot  $(\partial W/\partial I_1 + \lambda_2^2 \partial W/\partial I_2)$  against  $I_2$  for  $\lambda_2 = 1$  and  $\lambda_2 = 0.776$  from tables 3 and 4 respectively as shown in figure 9. We see that  $(\partial W/\partial I_1 + \lambda_2^2 \partial W/\partial I_2)$  decreases more rapidly, as  $I_2$  increases from 3.5 to 6.0, for  $\lambda_2 = 1$  than for  $\lambda_2 = 0.776$ . Also, we note that  $(\partial W/\partial I_1 + \lambda_2^2 \partial W/\partial I_2)$  decreases less and less rapidly as  $I_2$  increases for both values of  $\lambda_2$ . It will be seen in §§ 16 and 18 that these variations are in accord with the results of experiments on simple torsion and of those in which the simple torsion is superposed on a simple elongation.

It is seen from curve II of figure 9 that  $(\partial W/\partial I_1 + \lambda_2^2 \partial W/\partial I_2)$  increases with  $I_2$  at the larger values of  $I_2$  covered by the experiment. This effect is probably associated with the onset of crystallization in the rubber and can be seen in a more marked form in the experiment on simple extension (figure 10). If we employ a value of  $\frac{1}{8}$  for the ratio  $(\partial W/\partial I_2)/(\partial W/\partial I_1)$  when

TABLE 3

$N$ (kg.)	$\lambda_1$	$\frac{\partial W}{\partial I_1} + \frac{\partial W}{\partial I_2}$ (kg./cm. <sup>2</sup> )	$I_2$ (= $\bar{I}_1$ )
1.826	1.148	2.31	3.077
2.326	1.200	2.31	3.134
2.826	1.265	2.26	3.225
3.326	1.332	2.26	3.338
3.826	1.409	2.25	3.490
4.326	1.509	2.19	3.717
4.826	1.611	2.17	3.980
5.326	1.730	2.14	4.327
5.826	1.876	2.09	4.802
6.326	2.026	2.05	5.349
6.826	2.180	2.02	5.962
7.326	2.339	2.00	6.654
7.826	2.496	1.99	7.390
8.326	2.646	1.98	8.145
8.826	2.793	1.98	8.928
9.326	2.933	1.99	9.719
9.826	3.069	1.99	10.525

TABLE 4

$N$ (kg.)	$\lambda_1$	$\frac{\partial W}{\partial I_1} + \lambda_2^2 \frac{\partial W}{\partial I_2}$ ( $\lambda_2 = 0.776$ ) (kg./cm. <sup>2</sup> )	$I_1$	$I_2$
4.326	1.620	2.13	3.859	3.622
4.826	1.718	2.10	4.116	3.777
5.326	1.829	2.07	4.444	3.974
5.826	1.944	2.05	4.821	4.202
6.326	2.074	2.03	5.290	4.483
6.826	2.205	2.01	5.806	4.794
7.326	2.356	1.99	6.452	5.183
7.826	2.487	1.97	7.056	5.546
8.326	2.626	1.98	7.739	5.957
8.826	2.765	1.99	8.465	6.394
9.326	2.903	1.99	9.227	6.854
9.826	3.054	1.98	10.107	7.383

TABLE 5

$I_2$	3.75	4.00	4.25	4.50	4.75	5.00	5.25
$\left(\frac{\partial W}{\partial I_1} + 0.602 \frac{\partial W}{\partial I_2}\right)$ calculated (in kg./cm. <sup>2</sup> )	2.06	2.04	2.02	2.01	2.00	1.98	1.97
$\left(\frac{\partial W}{\partial I_1} + 0.602 \frac{\partial W}{\partial I_2}\right)$ measured (in kg./cm. <sup>2</sup> )	2.11	2.07	2.04	2.02	2.01	1.99	1.98

$I_2 = 5$ , as is suggested by the results given in §4, we obtain from curve I of figure 9,  $\partial W/\partial I_1 = 1.84$  kg./cm.<sup>2</sup> and  $\partial W/\partial I_2 = 0.23$  kg./cm.<sup>2</sup>. Now, assuming that  $\partial W/\partial I_1$  is constant and that  $\partial W/\partial I_2$  depends only on  $I_2$ , we obtain from curve I of figure 9 the value of  $\partial W/\partial I_2$  corresponding to any value of  $I_2$  by subtracting 1.84 from the corresponding value of



$(\partial W/\partial I_1 + \partial W/\partial I_2)$  given by the curve. From these values of  $\partial W/\partial I_2$  and the value  $1.84 \text{ kg./cm.}^2$  for  $\partial W/\partial I_1$ , we can calculate the values of  $(\partial W/\partial I_1 + 0.602 \partial W/\partial I_2)$  for various values of  $I_2$ . These calculated values are compared with the measured values, given by curve II of figure 9, in table 5. The agreement obtained is certainly within experimental error.

### 9. EXPERIMENT ON SIMPLE EXTENSION

In this experiment, the test-piece used consisted of a strip of vulcanized rubber  $A$ , about 5 cm. long and 0.8 cm. wide, cut from the same sheet as the test-pieces used in the experiments on pure shear and simple extension superposed on pure shear described in §§ 6 and 7 respectively. The thickness of the specimen, taken as the mean of the thicknesses measured at a number of points on it, was 0.86 mm.

Two fine lines, about 1 cm. apart, were drawn in ink on the test-piece perpendicular to its length and symmetrically placed with respect to its ends. In order that these lines should be as fine as possible, they were drawn with the test-piece in a highly extended state.

The ends of the test-piece were held firmly in metal clamps and suspended vertically from one of these clamps. Weights were successively added to the lower clamp, and the corresponding distances between the lines drawn on the test-piece were measured by means of a cathetometer. The distance between the marks, with the strip unstretched, was found by extrapolating to zero load the load-distance curve. The extension ratios  $\lambda$  corresponding to the various loads  $N$  were then calculated. In a subsidiary experiment, a check was made on the uniformity of the deformation in the region between the two fine lines, by subdividing this region and measuring the lengths between successive marks for various overall extensions.

### 10. RESULTS OF THE EXPERIMENT ON SIMPLE EXTENSION

In table 6 are given the results of the experiment on simple extension described in the previous section. In the first and second columns, corresponding values of the load  $N$  and extension ratio  $\lambda$  are given. From these and the cross-sectional area of the test-piece,

TABLE 6

$N$ (g.)	$\lambda$	$I_2$	$\frac{\partial W}{\partial I_1} + \frac{1}{\lambda} \frac{\partial W}{\partial I_2}$ (kg./cm. <sup>2</sup> )
58	1.056	3.009	2.60
108	1.119	3.037	2.41
158	1.192	3.088	2.31
208	1.270	3.158	2.28
258	1.364	3.265	2.23
308	1.478	3.414	2.15
358	1.613	3.610	2.08
408	1.769	3.854	2.00
458	1.939	4.144	1.95
508	2.121	4.465	1.91
558	2.305	4.797	1.88
608	2.506	5.171	1.85
658	2.686	5.510	1.84
708	2.874	5.869	1.83
758	3.056	6.219	1.83
808	3.225	6.546	1.84
858	3.383	6.854	1.86
908	3.525	7.131	1.88
958	3.680	7.434	1.90

$[\partial W/\partial I_1 + (1/\lambda) \partial W/\partial I_2]$  is calculated from equation (5.3), and the values obtained are given in the last column of the table and plotted against  $1/\lambda$  in figure 10.

In § 8 it has been seen how, assuming that  $\partial W/\partial I_1$  is constant and  $\partial W/\partial I_2$  is a function of  $I_2$  only, the values of  $\partial W/\partial I_1$  and of  $\partial W/\partial I_2$  at any specified value of  $I_2$  can be calculated from curve I of figure 9 (obtained from the experiments on pure shear). From the values so obtained, the value of  $[\partial W/\partial I_1 + (1/\lambda) \partial W/\partial I_2]$  can be calculated for any specified value of

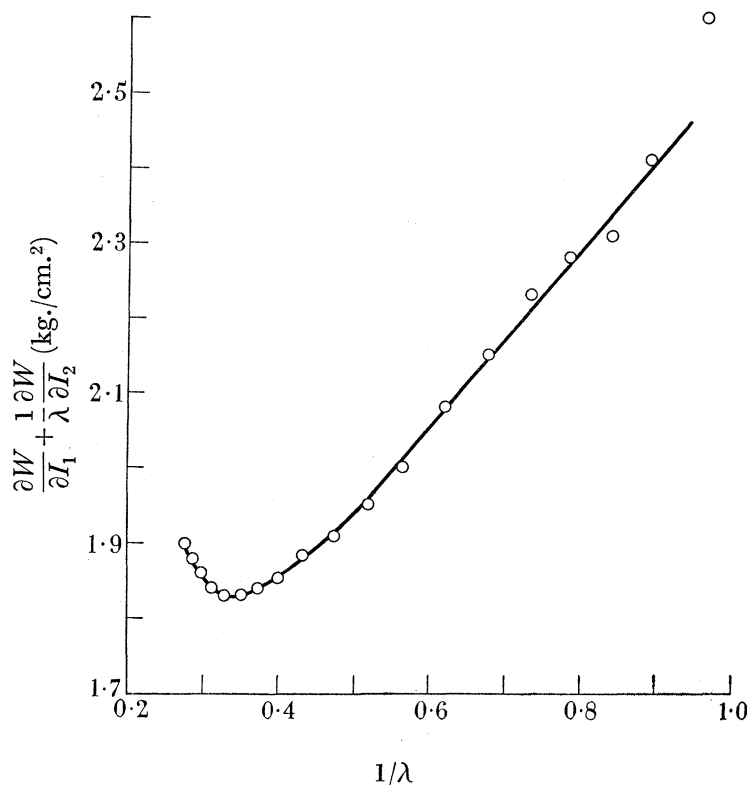


FIGURE 10. Plot of  $[\partial W/\partial I_1 + (1/\lambda) \partial W/\partial I_2]$  against  $1/\lambda$  from experiment on simple extension.

TABLE 7

$I_2$	3.2	3.6	4.0	4.4	4.8	5.2
$\left(\frac{\partial W}{\partial I_1} + \frac{1}{\lambda} \frac{\partial W}{\partial I_2}\right)$ calculated (in kg./cm. <sup>2</sup> )	2.18	2.08	2.02	1.98	1.94	1.92
$\left(\frac{\partial W}{\partial I_1} + \frac{1}{\lambda} \frac{\partial W}{\partial I_2}\right)$ measured (in kg./cm. <sup>2</sup> )	2.24	2.08	1.96	1.92	1.88	1.85

$I_2$ , within the range of values of  $I_2$  covered by the experiment on pure shear. In table 7 the values for  $[\partial W/\partial I_1 + (1/\lambda) \partial W/\partial I_2]$  obtained in this experiment on simple extension for various values of  $\lambda$  (i.e. of  $I_2$ ) are compared with the values calculated from the experiment on pure shear, in the manner described above. The agreement is seen to be within experimental error.

From figure 10 it is seen that the relation between  $[\partial W/\partial I_1 + (1/\lambda) \partial W/\partial I_2]$  and  $1/\lambda$  is very nearly linear over the range of values of  $1/\lambda$  from 0.9 to 0.45, i.e. for values of  $I_2$  from 3.03 to 4.65. The departure from linearity which occurs at values of  $1/\lambda$  below about 0.45 is probably due predominantly to crystallization.

At first sight we might be tempted to interpret the substantially linear portion of the curve in figure 10 as indicating that the rubber has a stored-energy function of the Mooney form (1.3), so that  $\partial W/\partial I_1$  and  $\partial W/\partial I_2$  are both constants,  $C_{10}$  and  $C_{01}$  respectively. If we make this interpretation and calculate the ratio  $C_{01}/C_{10}$  from the slope of the linear portion of the curve in figure 10 and its intercept on the axis  $1/\lambda = 1$ , we find that  $C_{01}/C_{10} \approx 0.8$ . Such an interpretation would lead to the prediction of constant values for  $(\partial W/\partial I_1 + \partial W/\partial I_2)$  in the experiment on pure shear and for  $(\partial W/\partial I_1 + 0.602 \partial W/\partial I_2)$  in the experiment in which a pure shear is superposed on a simple extension, at any rate over the ranges of values of  $I_1$  and  $I_2$  covered by the simple extension experiment. It is readily seen from figure 9 that the experimental results obtained for these deformations are not in accord with such predictions. Moreover, the value of  $C_{01}/C_{10}$  of about 0.8 disagrees with the value obtained from the experiments on two-dimensional deformation, the results of which are given in §4. It will also be seen that such an interpretation of the linear portion of the curve in figure 10 would be out of accord with the results of experiments on simple torsion.

## B. EXPERIMENT ON COMPRESSION

### 11. THEORETICAL CONSIDERATIONS

If the highly elastic sheet considered in §2, which has its major surfaces normal to the  $z$ -axis, is subjected to a pure homogeneous deformation for which the extension ratios  $\lambda_1$  and  $\lambda_2$  in the directions of the  $x$ - and  $y$ -axes are equal, then, employing the notation  $\lambda_1 = \lambda_2 = \lambda$ , the incompressibility condition  $\lambda_1 \lambda_2 \lambda_3 = 1$  yields  $\lambda_3 = 1/\lambda^2$ . The principal components of stress  $t_1$ ,  $t_2$  and  $t_3$  are given, from equations (2.1), by

$$\left. \begin{aligned} t_1 = t_2 &= 2 \left( \lambda^2 \frac{\partial W}{\partial I_1} - \frac{1}{\lambda^2} \frac{\partial W}{\partial I_2} \right) + p \\ t_3 &= 2 \left( \frac{1}{\lambda^4} \frac{\partial W}{\partial I_1} - \lambda^4 \frac{\partial W}{\partial I_2} \right) + p, \end{aligned} \right\} \quad (11.1)$$

and

where, from (2.5),

$$I_1 = 2\lambda^2 + \frac{1}{\lambda^4} \quad \text{and} \quad I_2 = \frac{2}{\lambda^2} + \lambda^4. \quad (11.2)$$

If the major surfaces of the sheet are force-free, then  $t_3 = 0$  and equations (11.1) yield

$$t_1 = t_2 = 2 \left( \lambda^2 - \frac{1}{\lambda^4} \right) \left( \frac{\partial W}{\partial I_1} + \lambda^2 \frac{\partial W}{\partial I_2} \right). \quad (11.3)$$

It may be noted that the same state of strain may be maintained by the stress system given by  $t_1 = t_2 = 0$  and  $t_3 = -2(\lambda^2 - 1/\lambda^4) (\partial W/\partial I_1 + \lambda^2 \partial W/\partial I_2)$ , where  $I_1$  and  $I_2$  are given by equations (11.2). This involves the application of a compressive force parallel to the  $z$ -axis. It is therefore evident that a measurement of  $t_1$  or  $t_2$  enables us to determine the stress associated with a simple compression of the material of extension ratio  $1/\lambda^2$ .

Deformations of the type considered, for which  $\lambda > 1$ , can be conveniently obtained experimentally (Treloar 1944) by inflating a thin circular sheet of rubber of uniform thickness, by applying an air pressure  $P$  under one of its faces. Then, the radial tension  $T$  at the

pole of the inflated sheet, measured per unit length on the major surface of the sheet in its deformed state, is related to the pressure  $P$  by the formula

$$P = \frac{2T}{r}, \quad (11.4)$$

where  $r$  is the radius of curvature at the pole. Let the initial thickness of the sheet be  $h$ . Then its thickness at its pole in the deformed state is  $h/\lambda^2$ . Provided that  $h \ll r$ , the components of stress at the pole are very nearly uniform across the thickness of the sheet and are given by equation (11.3) and  $t_3 = 0$ , if the  $z$ -axis of the reference system is taken along the normal to the sheet at its pole.

Writing  $t = t_1 = t_2$ , we have

$$T = \frac{th}{\lambda^2}, \quad (11.5)$$

so that, with (11.3),

$$P = \frac{4h}{r} \left(1 - \frac{1}{\lambda^6}\right) \left(\frac{\partial W}{\partial I_1} + \lambda^2 \frac{\partial W}{\partial I_2}\right), \quad (11.6)$$

$I_1$  and  $I_2$  being given by (11.2).

## 12. DESCRIPTION OF THE EXPERIMENT

A square test-piece of about 10 cm. edge was cut from a sheet of vulcanized rubber  $B$  of thickness 0.170 cm. The test-piece was clamped horizontally on its major surfaces between two brass plates, the upper of which had in it a circular hole of radius 2.5 cm. and the lower of which carried a tube. By pumping air into this tube, the sheet could be inflated, the air pressure being measured by a mercury manometer. The general arrangement is shown diagrammatically in figure 11. A suitable self-vulcanizing rubber solution was painted on the gripping surfaces of the clamp to act as an air seal and increase the friction between the test-piece and the clamp.

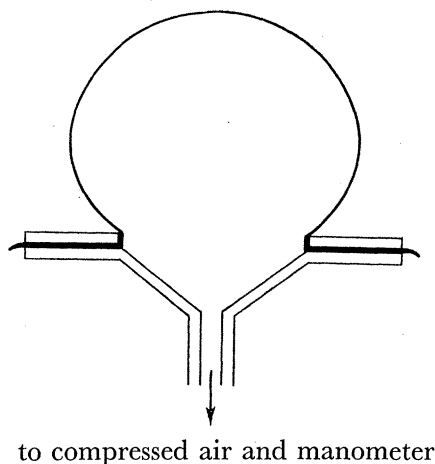


FIGURE 11. Experimental arrangement for experiment on simple compression.

The extension ratio at the pole of the inflated sheet was measured in the following manner. On the undeformed sheet two perpendicular straight lines  $A'A''$  and  $B'B''$  passing through the centre  $A_0$  were drawn, as shown in figure 12. Two lines  $C'C''$  and  $D'D''$ , parallel to  $A'A''$  and approximately  $\frac{1}{2}$  cm. from it, were drawn on either side of it, intersecting  $B'B''$  in  $C_0$  and  $D_0$ .

We shall call the points to which  $C_0$ ,  $A_0$  and  $D_0$  move in the deformation  $C$ ,  $A$  and  $D$  respectively. In each deformed state of the sheet, the horizontal and vertical projections of  $AC$  and  $AD$  were measured by means of a cathetometer having both horizontal and vertical travels and, from these, the extension ratios at the pole of the inflated sheet were calculated in the manner described below. We shall denote the horizontal projections of  $AC$  and  $AD$  by  $x_1$  and  $x_2$  respectively and their vertical projections by  $y_1$  and  $y_2$  respectively.

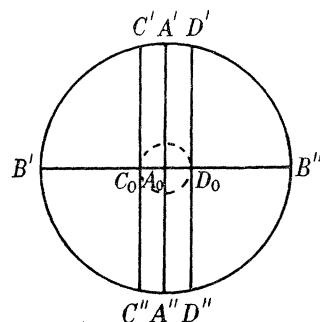


FIGURE 12. Test-piece for experiment on simple compression.

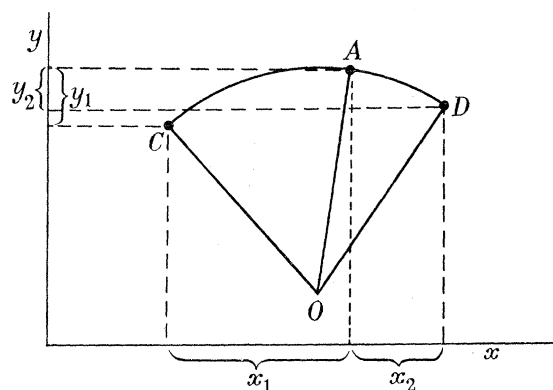


FIGURE 13. Geometrical considerations in the experiment on simple compression.

It was assumed that (i) the region of the sheet which in the undeformed state was a circle having its centre at  $A_0$  and radius about  $\frac{1}{2}$  cm., i.e. the region bounded by the broken line in figure 12, deformed into part of the surface of a sphere, the centre of which is  $O$  (say), and that (ii) the deformed sheet in this region has cylindrical symmetry about the normal to it at its pole. In carrying out the experiment it was necessary to choose a sheet of rubber which was sufficiently uniform in thickness and in its elastic properties for this assumption, that the deformed sheet has cylindrical symmetry, to be valid. It was not assumed that  $A$  is of necessity the pole of the deformed sheet, although it will be seen from the experimental results that this is very nearly the case. If these assumptions are valid for the deformation, then the straight line  $C_0D_0$  on the undeformed sheet deforms into the arc of a circle  $CAD$ , the centre of which is  $O$ , as shown in figure 13. Now, let  $P_0$  be an arbitrary point on  $C_0D_0$  and let  $P$  be the position on the circle  $CAD$  of this point when the sheet is deformed. Let  $ds$  be an element of length of  $C_0D_0$  at  $P_0$ , and let  $ds'$  be the corresponding element of length in the deformed state of the sheet. Then, provided that the extension ratio  $(ds'/ds) = \lambda$  is nearly constant for all positions of  $P$  on  $CAD$ , its magnitude at the pole is given by (length of arc  $CD$ )/ $C_0D_0$ .



The radius of curvature  $r$  ( $= OA$ ) can then be calculated from the measurements  $x_1, x_2, y_1$  and  $y_2$  by means of the formula

$$r^2 = \frac{\frac{1}{4}(x_1^2 + y_1^2)(x_2^2 + y_2^2)[(x_1 + x_2)^2 + (y_1 - y_2)^2]}{(x_1 y_2 + y_1 x_2)^2}. \quad (12.1)$$

The extension ratio  $\lambda$  may then be calculated from the formula

$$\lambda = r\theta/l, \quad (12.2)$$

where  $l = C_0 D_0$  and  $\theta$  denotes the angle  $COD$ , measured in radians.  $\theta$  is given in terms of  $x_1, x_2, y_1$  and  $y_2$  by the formula

$$\theta = 2 \sin^{-1} \frac{1}{2r} [(x_1 + x_2)^2 + (y_1 - y_2)^2]^{\frac{1}{2}}. \quad (12.3)$$

The formulae (12.1), (12.2) and (12.3) can be readily obtained by simple geometrical considerations from figure 13. It will be seen from table 8, in which are given the values of  $x_1, x_2, y_1$  and  $y_2$  found experimentally for various values of the inflating pressure  $P$ , that  $(y_1 - y_2)$  is negligibly small compared with  $(x_1 + x_2)$ , so that equations (12.1) and (12.3) may be written as

$$r = \frac{1}{2} \frac{x_1 + x_2}{x_1 y_2 + y_1 x_2} [(x_1^2 + y_1^2)(x_2^2 + y_2^2)]^{\frac{1}{2}} \quad (12.4)$$

and

$$\theta = 2 \sin^{-1} \frac{x_1 + x_2}{2r}. \quad (12.5)$$

Now, it is clear that, particularly for low values of  $P$  when the values of  $y_1$  and  $y_2$  are small and therefore subject to a large experimental error, the values of  $r$ , found from equation (12.4), are correspondingly inaccurate. It is therefore desirable to eliminate  $r$  from equation (12.2) for determining  $\lambda$ . It is noted that  $(x_1 + x_2)/2r$  is always less than  $\frac{1}{2}$ . Consequently equation (12.5) can, with sufficient accuracy, be written

$$\theta = \frac{x_1 + x_2}{r} \left[ 1 + \frac{1}{24} \left( \frac{x_1 + x_2}{r} \right)^2 \right]. \quad (12.6)$$

Introducing this expression for  $\theta$  into (12.2), we obtain

$$\lambda = \frac{x_1 + x_2}{l} \left[ 1 + \frac{1}{24} \left( \frac{x_1 + x_2}{r} \right)^2 \right]. \quad (12.7)$$

Since the term  $[(x_1 + x_2)/r]^2$  is in all cases a small correcting term, the inaccuracy of  $r$  is of no disadvantage.

### 13. EXPERIMENTAL RESULTS

In the first five columns of table 8 are given corresponding values of the inflating pressure  $P$  in mm. of mercury and  $x_1, x_2, y_1$  and  $y_2$ . In the sixth and seventh columns are given the values of  $r$  and  $\lambda^2$  calculated from equations (12.4) and (12.7) respectively, employing the measured value of  $l = 1.02$  cm. From these values of  $\lambda^2$ ,  $I_1 - 3$  and  $I_2 - 3$  are calculated by means of equations (11.2), and the values obtained are given in the eighth and ninth columns. In the last column the corresponding values of  $Pr/4h(1 - \lambda^{-6})$  are given. These are calculated from the figures given in the preceding columns, using the measured value of  $h = 0.170$  cm. The values of  $Pr/4h(1 - \lambda^{-6})$  for values of  $\lambda$  only slightly different from unity are very inaccurate owing to the inaccuracy of both  $r$  and  $(1 - \lambda^{-6})$  in this region.

It is seen from equation (11.6) that writing  $\lambda^2 = 1/\lambda'$

$$\frac{Pr}{4h(1-\lambda^{-6})} = \frac{\partial W}{\partial I_1} + \frac{1}{\lambda'} \frac{\partial W}{\partial I_2}, \quad (13.1)$$

where, from (11.2),

$$I_1 = \frac{2}{\lambda'} + \lambda'^2 \quad \text{and} \quad I_2 = 2\lambda' + \frac{1}{\lambda'^2}. \quad (13.2)$$

From table 8  $[\partial W/\partial I_1 + (1/\lambda') \partial W/\partial I_2]$  is plotted against  $1/\lambda'$  in figure 14, as the curve for which  $1/\lambda' > 1$ . For purposes of comparison, values of  $[\partial W/\partial I_1 + (1/\lambda') \partial W/\partial I_2]$  obtained from an experiment on simple extension (extension ratio  $\lambda'$ ) are plotted on the same graph. The experiment was performed in the manner described in § 9 using a test-piece cut from the same sheet as the test-piece employed for the inflation experiment.

TABLE 8

<i>P</i> (mm. of mercury)	<i>x</i> <sub>1</sub> (cm.)	<i>x</i> <sub>2</sub> (cm.)	<i>y</i> <sub>1</sub> (cm.)	<i>y</i> <sub>2</sub> (cm.)	<i>r</i> (cm.)	$\lambda^2$	<i>I</i> <sub>1</sub> -3	<i>I</i> <sub>2</sub> -3	$\frac{Pr}{4h(1-\lambda^{-6})}$ (kg./cm. <sup>2</sup> )
85	0.56	0.55	0.04	0.04	4	1.19	0.08	0.10	1.7
151	0.61	0.56	0.05	0.04	4	1.32	0.21	0.26	2.1
205	0.64	0.60	0.06	0.06	3.3	1.51	0.46	0.60	1.9
266	0.69	0.66	0.07	0.09	2.9	1.77	0.86	1.26	1.87
298	0.75	0.72	0.10	0.10	2.7	2.10	1.43	2.36	1.80
329	0.89	0.85	0.16	0.16	2.5	3.03	3.17	6.84	1.70
334	1.06	1.03	0.22	0.23	2.55	4.37	5.8	16.5	1.72
325	1.32	1.28	0.37	0.34	2.55	7.0	11	46	1.66
316	1.48	1.42	0.41	0.42	2.72	8.9	15	76	1.71
308	1.59	1.54	0.48	0.46	2.84	10.3	17.5	103	1.74
301	1.72	1.65	0.50	0.50	3.07	12.0	21	141	1.85

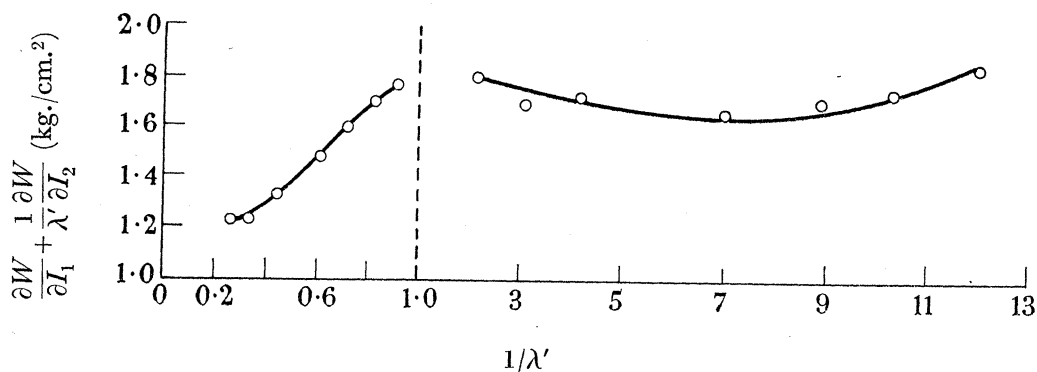


FIGURE 14. Plot of  $[\partial W/\partial I_1 + (1/\lambda') \partial W/\partial I_2]$  against  $1/\lambda'$  from experiments on simple compression and simple extension. (Note change of scale at  $1/\lambda' = 1$ .)

It is seen from figure 14 that for  $1/\lambda' \gg 1$ ,  $[\partial W/\partial I_1 + (1/\lambda') \partial W/\partial I_2]$  is approximately constant, and that the points are not on the same straight line as those for which  $1/\lambda' < 1$ . It can be seen, at any rate qualitatively, that this result is consistent with the behaviour of  $\partial W/\partial I_1$  and  $\partial W/\partial I_2$  deduced from the earlier experiments.

We see from equations (13.2) that when  $1/\lambda' = 0.5$ ,  $I_2 = 4.25$ . From curve I of figure 9,  $(\partial W/\partial I_2)/(\partial W/\partial I_1)$  can be calculated for this value of  $I_2$  as 0.16. We assume that the same value applies in the experiments at present under discussion, and note from figure 14 that when  $1/\lambda' = 0.5$ , so that  $I_2 = 4.25$ ,  $[\partial W/\partial I_1 + (1/\lambda') \partial W/\partial I_2] = 1.38$  kg./cm.<sup>2</sup>. From this we

obtain  $\partial W/\partial I_1 = 1.28$  and  $\partial W/\partial I_2 = 0.20$  when  $I_2 = 4.25$ . Assuming that the value of  $\partial W/\partial I_1$  remains constant, we can calculate the values of  $(\partial W/\partial I_2)/(\partial W/\partial I_1)$  for the whole range of values of  $I_2$  covered by the experiments. The results are given in table 9.

TABLE 9

$1/\lambda'$	0.5	0.6	0.7	0.8	3	5	7	9	11
$I_2$	4.25	3.69	3.35	3.14	9.67	25.4	49.3	81.2	121
$(\partial W/\partial I_2)/(\partial W/\partial I_1)$	0.16	0.26	0.33	0.39	0.12	0.06	0.04	0.03	0.035

It is seen that the manner in which  $(\partial W/\partial I_2)/(\partial W/\partial I_1)$  varies with  $I_2$  is very similar to that indicated by the experiments described in §§ 2 to 10. The more rapid fall of  $(\partial W/\partial I_2)/(\partial W/\partial I_1)$  with increase of  $I_2$  at the lower values of  $I_2$  than that obtained in the previous experiments may well result from the fact that the test-pieces used in the present experiments were prepared from a different rubber specimen than those employed in the earlier experiments.

In calculating the values of  $(\partial W/\partial I_2)/(\partial W/\partial I_1)$  given in table 9, we have taken over the value of this ratio at  $I_2 = 4.25$  from the experiment on pure shear conducted with a test-piece which has a different formulation. It is shown, however, in appendix 5 (§ 24) that a somewhat different choice of the value of  $(\partial W/\partial I_2)/(\partial W/\partial I_1)$  at  $I_2 = 4.25$  has relatively little effect on the values of this ratio calculated from the experimental results for very different values of  $I_2$ .

### C. EXPERIMENTS ON THE TORSION OF A CYLINDER

#### 14. BASIC FORMULAE

We consider a right-circular cylinder of length  $l_0$  and radius  $a$  in its undeformed state to be deformed in the following manner. It is first subjected to a simple extension in which its length increases to  $l (= \lambda l_0)$  and its radius decreases to  $\lambda^{-1/2}a$ . It is then subjected to a simple torsion in which circular cross-sections normal to the axis of the cylinder are rotated about the axis and in their own plane through an angle which is proportional to their distance from one end. The constant of proportionality  $\psi$  is termed the amount of torsion, and it is readily seen that the angle  $\theta$  through which one end of the cylinder is rotated with respect to the other is given by

$$\theta = \psi l = \psi \lambda l_0. \quad (14.1)$$

It has been shown (Rivlin 1949 *b*) that such a state of deformation can be produced by the application of surface tractions to the plane ends of the cylinder, and that these may be resolved into components which are normal and azimuthal to the surfaces on which they act in their deformed state. The resultant of the azimuthal components is a couple  $M$  given by

$$M = 4\pi\psi \int_0^a r^3 \left( \frac{\partial W}{\partial I_1} + \frac{1}{\lambda} \frac{\partial W}{\partial I_2} \right) dr, \quad (14.2)$$

and the resultant of the normal surface tractions is a longitudinal force  $N$  given by

$$N = 4\pi \left( \lambda - \frac{1}{\lambda^2} \right) \int_0^a r \left( \frac{\partial W}{\partial I_1} + \frac{1}{\lambda} \frac{\partial W}{\partial I_2} \right) dr - 2\pi\psi^2 \int_0^a r^3 \left( \frac{\partial W}{\partial I_1} + \frac{2}{\lambda} \frac{\partial W}{\partial I_2} \right) dr. \quad (14.3)$$

In equations (14.2) and (14.3),  $I_1$  and  $I_2$  are given by

$$I_1 = \lambda^2 + \frac{2}{\lambda} + \lambda\psi^2 r^2 \quad \text{and} \quad I_2 = 2\lambda + \frac{1}{\lambda^2} + \psi^2 r^2. \quad (14.4)$$

From equations (14.2) and (14.3), we have

$$\frac{[N]_{\psi=0} a^2}{[M/\psi]_{\psi=0}} = 2\left(\lambda - \frac{1}{\lambda^2}\right). \quad (14.5)$$

This means that the ratio between the load necessary to produce the simple extension ratio  $\lambda$  and the torsional modulus for infinitesimal torsions superposed on that simple extension is independent of the form of the stored-energy function.

If the cylinder is maintained unextended, so that  $\lambda = 1$ , equations (14.2) and (14.3) yield

$$M = 4\pi\psi \int_0^a r^3 \left( \frac{\partial W}{\partial I_1} + \frac{\partial W}{\partial I_2} \right) dr, \quad N = -2\pi\psi^2 \int_0^a r^3 \left( \frac{\partial W}{\partial I_1} + 2 \frac{\partial W}{\partial I_2} \right) dr, \quad (14.6)$$

while expressions (14.4) become 
$$I_1 = I_2 = 3 + \psi^2 r^2. \quad (14.7)$$

Thus, in order to produce a torsion of amount  $\psi$  in a right-circular cylinder of rubber, to the plane ends of which are bonded rigid plates, we must apply to these ends a couple  $M$  and a thrust  $-N$  parallel to the axis of the cylinder.

If the stored-energy function has the Mooney form (1.3) then equations (14.2) and (14.3) yield

$$\left. \begin{aligned} M &= \pi\psi a^4 [C_{10} + (1/\lambda) C_{01}] \\ \text{and} \quad N &= 2\pi a^2 [C_{10} + (1/\lambda) C_{01}] (\lambda - 1/\lambda^2) - \pi\psi^2 a^4 \left[ \frac{1}{2} C_{10} + (1/\lambda) C_{01} \right]. \end{aligned} \right\} \quad (14.8)$$

It is noted that, in this case, if  $M/\pi a^4 \psi$  is plotted against  $1/\lambda$  we obtain a straight line, the intercept of which on the line  $1/\lambda = 1$  is  $(C_{10} + C_{01})$  and slope of which is  $C_{01}$ .

Again, if  $\lambda = 1$ , equations (14.8) become

$$M = \pi a^4 \psi (C_{10} + C_{01}) \quad \text{and} \quad N = -\pi a^4 \psi^2 \left( \frac{1}{2} C_{10} + C_{01} \right). \quad (14.9)$$

It is noted that in this case, the couple  $M$  is proportional to the amount of torsion  $\psi$  and the total thrust  $-N$  to the square of this. If measurements of  $M$  and  $-N$  are made for various values of  $\psi$ , then the slope of the  $M$  against  $\psi$  curve gives a measurement of  $(C_{10} + C_{01})$  and that of the  $-N$  against  $\psi^2$  curve gives a measurement of  $(C_{10} + \frac{1}{2} C_{01})$ . From these values  $C_{01}/C_{10}$  can be calculated.

It will be appreciated that any departure of the  $M$  against  $\psi$  curve, or the  $-N$  against  $\psi^2$  curve, from linearity indicates a departure of the stored-energy function from the Mooney form.

In order to verify the formulae given in this section, two types of experiment were carried out. In the experiment described in §15 a cylinder of rubber was subjected to simple torsion, and the corresponding value of  $M$ ,  $-N$  and  $\psi$  were measured. In the experiments described in §17, a cylindrical rod of rubber was subjected simultaneously to simple extension and torsion, and for each value of  $\lambda$  corresponding values of  $M$  and  $\psi$  were measured, as well as the value of  $N$  when  $\psi = 0$ .

## 15. THE EXPERIMENT ON SIMPLE TORSION

The experiment was carried out with a vulcanized rubber cylinder of length 1 in. and diameter 1 in., bonded to mild steel end-plates 1 in. in diameter and  $\frac{3}{8}$  in. thick. The rubber cylinder was prepared according to the recipe *B* given in §20.



It was attached, by the end-plates bonded to it, to the circular plate  $P$  and a base-plate  $B$ , as shown in figure 15. A rod  $R$  was rigidly attached to  $P$  at its centre. The circular plate  $P$  and rod  $R$  weighed about 2 kg., and, together with the small trimming weight  $m$ , were counter-balanced by the load  $L$  through the string  $S$  passing over a pulley. The pulley was located in such a way that the string was vertical between it and the rod  $R$ . This method of counter-balancing was employed in order to minimize tilting of the plate  $P$  when the cylinder was subjected to a torque.

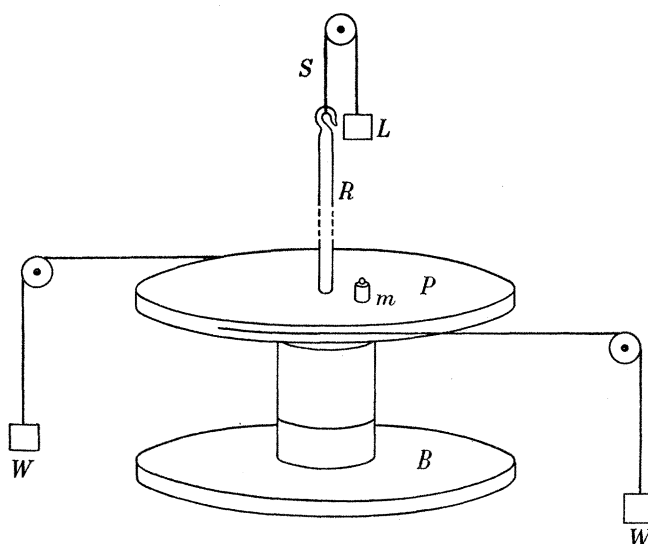


FIGURE 15. Experimental arrangement for experiment on torsion of a cylinder.

A known torque was applied to the rubber cylinder by strings, supporting equal weights  $W$ , the torque being varied by altering these. The strings were carried in a groove in the edge of the circular plate  $P$ .

As the torque was increased from zero, the cylinder elongated, and this elongation was observed by noting the rise or fall of two points on the edge of the plate  $P$  at opposite ends of a diameter, one cathetometer being used to observe each of the points. The plate  $P$  was kept horizontal, as judged by a bubble level, by suitable placing of the mass  $m$ . At each value of the applied torque, the magnitude of the counterpoise  $L$  which would result in no extension of the cylinder was found by measuring the extension and compression for values of  $L$  slightly greater and less than this value and interpolating. The difference between this value of  $L$  and that obtained for zero torque gives the value of the thrust  $-N$  corresponding to the particular value of the applied torque employed. The extensions and compressions were taken as the means of those measured with the two cathetometers at diametrically opposed points on the rim of the plate.

At each value of the applied torque, the amount of torsion produced was also measured by reading a scale on the edge of the plate  $P$  against a fiducial mark.

#### 16. RESULTS OF THE EXPERIMENT ON SIMPLE TORSION

The corresponding values of the applied torque  $M$  and amount of torsion  $\psi$  measured in the experiment are shown in figure 16, both for the case when the torque is steadily increased to its maximum value (curve I) and when it is decreased to zero (curve II). The small



amount of hysteresis may be noted. It is seen that the curve obtained is nearly linear, but that there is a slight curvature towards the  $\psi$ -axis.

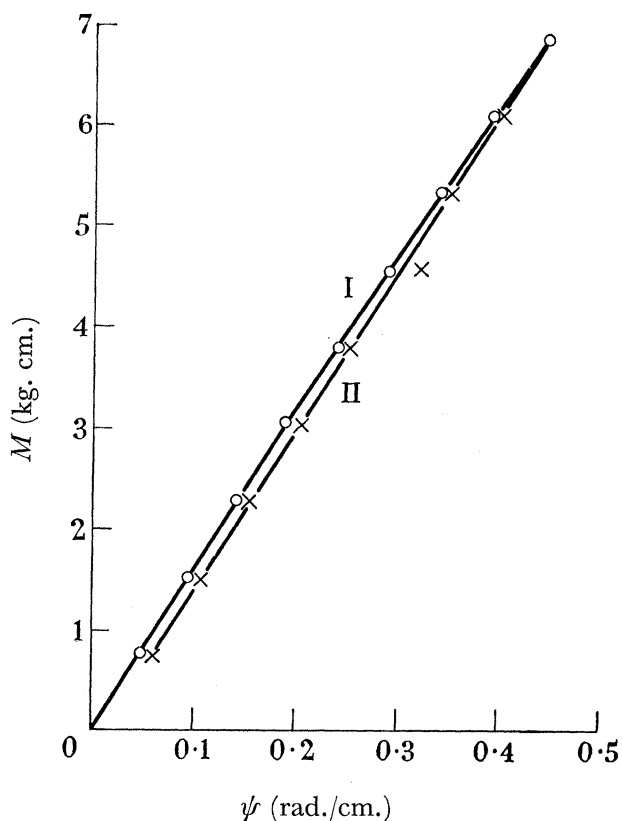


FIGURE 16. Plot of torsional couple  $M$  against amount of torsion  $\psi$ . I, load increasing; II, load decreasing.

In figure 17 the values of the total thrust  $-N$  obtained in the experiment are plotted against  $\psi^2$  both for the case of increasing (curve I) and decreasing (curve II) torque. The relation is seen to be linear in both cases within the accuracy of experimental error. It will be noted that both straight lines give a finite intercept on the  $-N$ -axis. Now, it is readily seen from the second of equations (14.6) that so long as the basic assumptions of the theory are satisfied, the value of  $-N$  corresponding to  $\psi = 0$  should be zero, whatever the form of the stored-energy function. This would, in general, no longer be the case if the material were anisotropic in the undeformed state. Any hysteresis or permanent set associated with the higher values of  $\psi$  would result in such anisotropy and may well explain the finite intercept on the  $-N$ -axis. This hypothesis is in accord with the observation that the intercept of the  $\psi$ -decreasing curve is greater than that of the  $\psi$ -increasing curve.

It has been pointed out in §1 (see also §21) that a stored-energy function of the Mooney form (1.3) will be applicable for sufficiently small deformations (i.e. for sufficiently small values of  $(I_1 - 3)$  and  $(I_2 - 3)$ ). The approximate linearity of the  $M$  against  $\psi$  and of the  $-N$  against  $\psi^2$  curves suggests that  $\partial W/\partial I_1$  and  $\partial W/\partial I_2$  are indeed nearly constant over the range of values of  $I_1$  and  $I_2$  (3 to 3.32)\* covered by the experiment, so that the Mooney form (1.3)

\* It will be appreciated that in any state of torsion of the cylinder,  $I_1$  and  $I_2$  vary along the radius of the cylinder from 3 on its axis to a maximum on its curved surface. The values given are those at the curved surface.

for the stored-energy function is approximately applicable, at any rate for the smaller values of  $\psi$ . The appropriate value of  $C_{01}/C_{10}$  which is seen to be the value of  $(\partial W/\partial I_2)/(\partial W/\partial I_1)$  when  $I_1 = I_2 = 3$  can be calculated, by the method outlined in § 14, from the experimental results given in figures 16 and 17. In carrying out this calculation, the value of  $M/\psi$  was obtained by taking the slope at  $\psi = 0$  of curve I of figure 16 (i.e. the slope of the broken line) and that of  $-N/\psi^2$  by taking the slope of the straight line I in figure 17. The value of  $C_{01}/C_{10}$  so calculated was  $\frac{1}{3}$ , which is in reasonable agreement with the value given for  $(\partial W/\partial I_2)/(\partial W/\partial I_1)$  at  $I_1 = I_2 = 3$  for a similar rubber, in table 9.

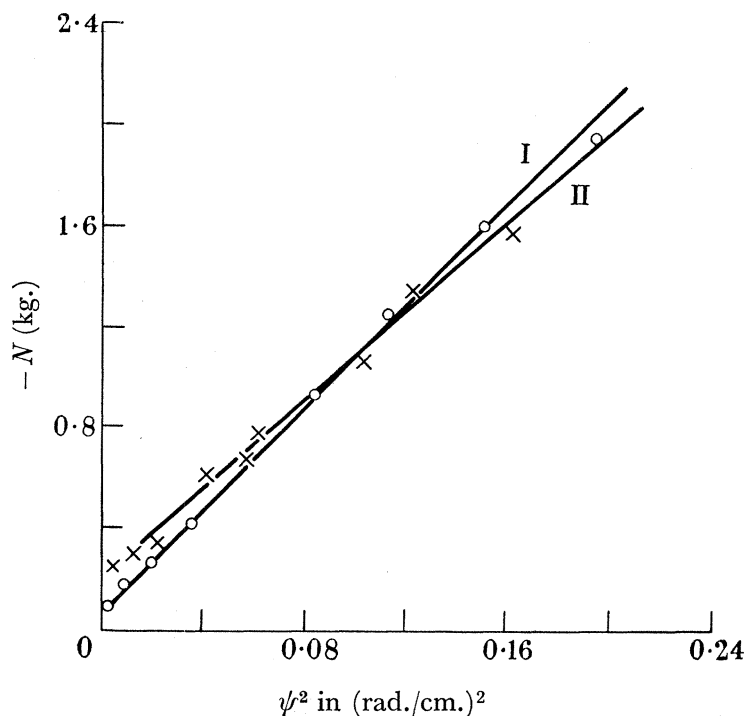


FIGURE 17. Plot of normal force  $-N$  against  $\psi^2$ . I, load increasing; II, load decreasing.

It should be noted, however, that the experimental results given in figures 16 and 17 are rather insensitive to the value of  $C_{01}/C_{10}$ . As an illustration,  $C_{01}/C_{10}$  was calculated from the slopes of curves II in figures 16 and 17, and the value  $\frac{1}{3}$  was obtained.

The slight departure from linearity of the  $M$  against  $\psi^2$  curve is in accord with the fall of  $\partial W/\partial I_2$  with increase in  $I_2$  observed in the earlier experiments. This point is, however, more conveniently discussed in connexion with the series of experiments dealt with in the following sections.

In a previous paper (Rivlin 1947) the distribution of the normal force  $Z$  over the plane end of a circular cylinder of rubber subjected to simple torsion was measured as a function of the amount of torsion  $\psi$ . Within experimental error, the results appeared to be in accord with a stored-energy function of the Mooney form (1.3) in which  $C_{01}/C_{10} = \frac{1}{7}$ . The experimental errors were such that a small departure from constancy in  $C_{10}$  or  $C_{01}$  would not be detectable, but the method was, unlike that described in the foregoing section, very suitable for the determination of  $C_{01}/C_{10}$ . The range of values of  $I_1$  and  $I_2$  covered in the experiment was 3 to 4. If the ratio  $(\partial W/\partial I_2)/(\partial W/\partial I_1)$  varied slightly over this range of values of  $I_1$  and  $I_2$ , the ratio  $C_{01}/C_{10}$  found in the experiment should be interpreted as a mean value of

$(\partial W/\partial I_2)/(\partial W/\partial I_1)$  over this range. It is seen that the value of  $\frac{1}{7}$  is in reasonably good agreement with that given by the experiment on pure shear which yields (§8) a value of about  $\frac{1}{5}$  for this ratio at  $I_2 = 3.5$ . It should be noted, however, that the test-piece employed in the earlier experiment was prepared according to a different recipe from those used in the experiments described in this paper. The experiment was therefore repeated using recipe *B* and a similar apparent value for  $C_{01}/C_{10}$  was obtained.

#### 17. THE EXPERIMENTS ON COMBINED TORSION AND SIMPLE EXTENSION

In order to verify the applicability of the relations derived in §14 for the forces associated with combined torsion and simple extension, a cylindrical rubber test-piece,  $\frac{3}{8}$  in. in diameter and 3 in. in length, prepared according to the recipe *A* (see §20), was subjected to various constant extensions. At each value of the extension ratio  $\lambda$  the dependence of the torque  $M$  on the amount of torsion  $\psi$  was measured. The longitudinal force  $[N]_{\psi=0}$  necessary to produce the simple extension was also measured for each value of  $\lambda$  under the condition of zero amount of torsion.

The apparatus used is shown diagrammatically in figure 18.

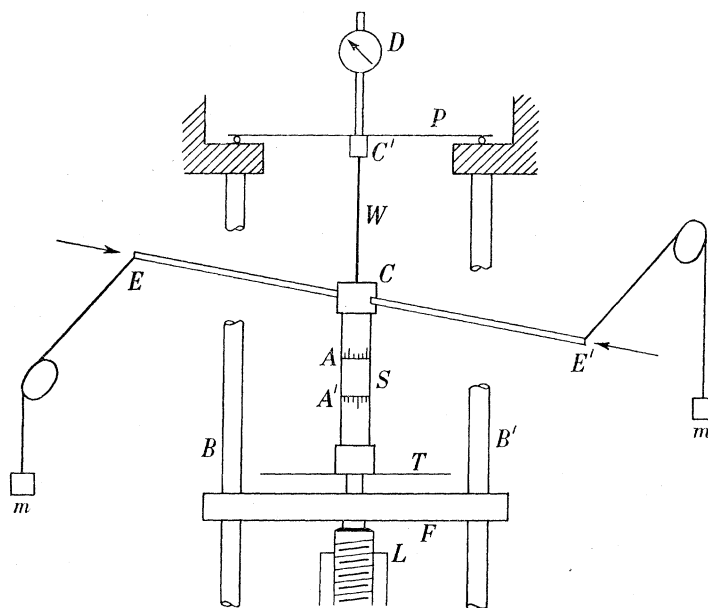


FIGURE 18. Experimental arrangement for experiment on torsion superposed on simple extension.

It consisted essentially of a calibrated plate spring *P* supported horizontally by two rollers on a rigid casting. To the centre of the spring, a vertical wire *W* was attached by a suitable clamp *C'*. A clamp *C* at the lower end of the wire supported a light torque arm *EE'* and the cylindrical rubber test-piece *S*. This had rigid steel disks  $\frac{3}{8}$  in. in diameter bonded to its ends. By the upper of these it was held in the clamp *C* in a vertical position. The lower end of the test-piece was attached rigidly, by the steel disk bonded to it, to the torsion head *T*, which was in turn attached to the horizontal bar *F* which could slide up or down on the vertical guide rails *B* and *B'*, its movement being controlled by the screw *L*. By means of these any desired extension could be produced in the test-piece.

Strings were attached to the ends of the torque arm *EE'*, and these passed over pulleys

and carried equal weights  $m$ . The positions of the pulleys were such that the strings were in a horizontal plane and, in the 'zero' position of the torque arm  $EE'$ , when the wire  $W$  was subject to no torsion, the strings were at right angles to the torque arm. The torque was varied by altering the weights  $m$  and, for each value of these, the torsion head  $T$  was turned until the torque arm  $EE'$  was in its zero position.

The rubber cylinder had moulded on it a grid of longitudinal and circumferential lines, obtained by engraving the mould in which the test-piece was made. The extension ratio was obtained by measuring with a cathetometer the distances between two of the circumferential lines  $A$  and  $B$ , about 3 cm. apart when the test-piece was undeformed and symmetrically disposed about its centre. Denoting by  $l$  and  $l_0$  the distances between  $A$  and  $B$  in the deformed and undeformed states respectively, the corresponding extension ratio  $\lambda$  is, of course, given by  $l/l_0$ . The value of  $l_0$  was not obtained by direct measurement for zero load, but was found by measuring  $l$  for increasing values of the longitudinal load and extrapolating back to zero load.

In order to measure the amount of torsion  $\psi$  the angular scales formed by the intersections of the longitudinal lines of the grid with  $A$  and  $B$  were observed through a telescope having a vertical travel and containing cross-wires. The value of  $\psi$  is then given by  $\theta/l$ , where  $\theta$  is the difference, in radians, between the angles through which the scales  $A$  and  $B$  are rotated from their positions when the cylinder is subjected to no torque.

The longitudinal force was found by measuring the deflexion of the calibrated plate spring  $P$  by means of a dial gauge  $D$ . The deflexions of the spring were sufficiently small to have a negligible effect on the extension of the rubber test-piece.

## 18. EXPERIMENTAL RESULTS

The manner in which the torque  $M$  was found to depend on the amount of torsion  $\psi$  for various values of the extension ratio  $\lambda$  is shown in figure 19. It is seen that the curves for the lower values of  $\lambda$  depart from linearity and that this departure decreases with increase in  $\lambda$ .

The values of the total load  $N$  required to produce the various extensions at zero torsion ( $\psi = 0$ ) are given in table 10, together with the corresponding values of  $[\partial W/\partial I_1 + (1/\lambda)\partial W/\partial I_2]$  calculated from them by means of the formula

$$(N)_{\psi=0} = 2\pi a^2 \left( \lambda - \frac{1}{\lambda^2} \right) \left( \frac{\partial W}{\partial I_1} + \frac{1}{\lambda} \frac{\partial W}{\partial I_2} \right), \quad (18.1)$$

in which

$$I_1 = \lambda^2 + \frac{2}{\lambda} \quad \text{and} \quad I_2 = 2\lambda + \frac{1}{\lambda^2}. \quad (18.2)$$

TABLE 10

extension ratio $\lambda$	1.095	1.238	1.431	1.725	2.072	2.501
$(N)_{\psi=0}$ (kg.)	0.814	1.628	2.442	3.256	4.070	4.884
$\left( \frac{\partial W}{\partial I_1} + \frac{1}{\lambda} \frac{\partial W}{\partial I_2} \right)$ (kg./cm. <sup>2</sup> )	2.18	1.95	1.80	1.65	1.56	1.47

This formula can readily be obtained from equations (14.3) and (14.4). Again, from equations (14.2) and (14.4), we obtain

$$\left[ \frac{M}{\psi} \right]_{\psi=0} = \pi a^4 \left( \frac{\partial W}{\partial I_1} + \frac{1}{\lambda} \frac{\partial W}{\partial I_2} \right), \quad (18.3)$$

where  $I_1$  and  $I_2$  are given by (18.2).

From the values of  $[\partial W/\partial I_1 + (1/\lambda) \partial W/\partial I_2]$  given in table 10, we can calculate, by means of equation (18.3), the corresponding values of  $[M/\psi]_{\psi=0}$ . The broken lines in figure 19 represent the linear relation  $M = [M/\psi]_{\psi=0} \psi$  for each value of  $\lambda$ . These straight lines should, according

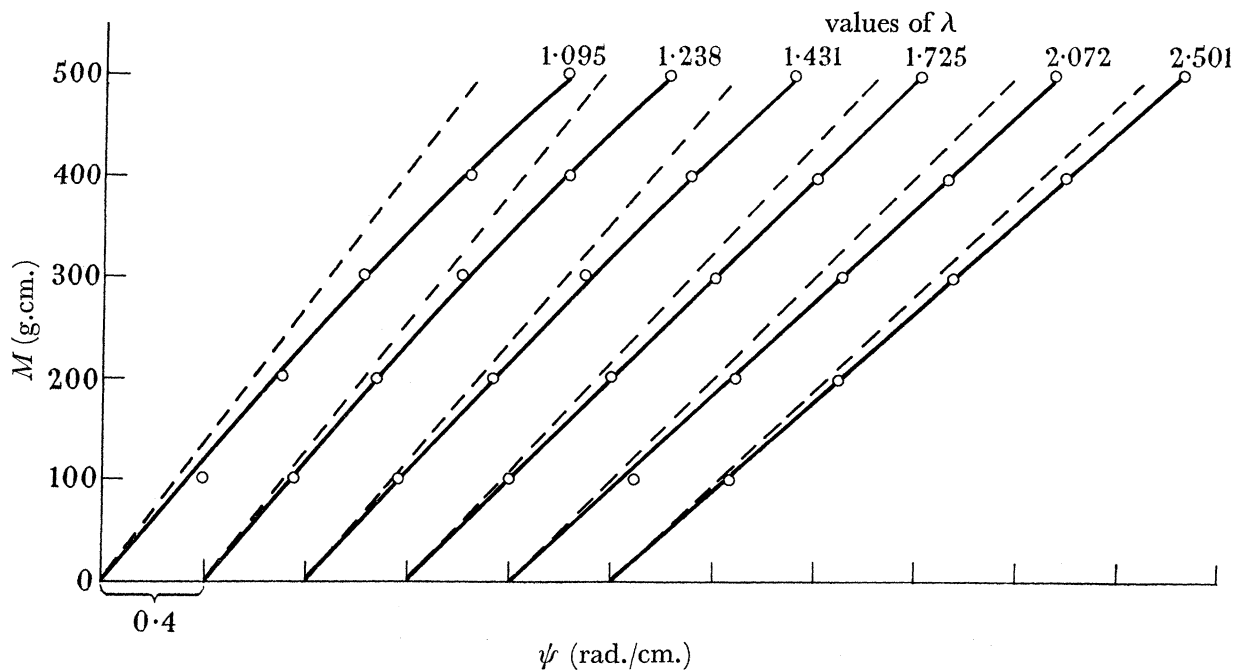


FIGURE 19. Plot of torsional couple  $M$  against amount of torsion  $\psi$  for various values of the extension ratio  $\lambda$  (large range of variation of  $\psi$ ; the origin is shifted by 0.4 unit parallel to the abscissa for each increment in the value of  $\lambda$ ).

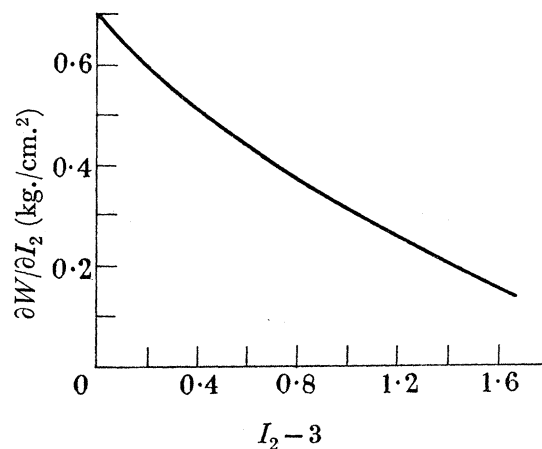


FIGURE 20. Plot of  $\partial W/\partial I_2$  against  $(I_2 - 3)$ .

to the theory, be tangential to the corresponding  $M$  against  $\psi$  curves at  $\psi = 0$ . Also the departure of the  $M$  against  $\psi$  curves from the straight lines at the larger values of  $\psi$  is to be explained by the fall of  $[\partial W/\partial I_1 + (1/\lambda) \partial W/\partial I_2]$  with increase of the deformation.

We can obtain an estimate of the amount of this departure for each of the  $M$  against  $\psi$  curves in the following manner. If the values of  $[\partial W/\partial I_1 + (1/\lambda) \partial W/\partial I_2]$  given in table 10 are plotted against  $1/\lambda$  they lead to a substantially linear relation (cf. figures 10 and 14 ( $1/\lambda' < 1$ )). If the assumptions are now made that  $\partial W/\partial I_1$  is constant, that  $\partial W/\partial I_2$  is independent



of  $I_1$  and that  $(\partial W/\partial I_2)/(\partial W/\partial I_1) = 0.16$  when  $I_2 = 4.25$  (corresponding to  $1/\lambda = 0.5$ ), then the value of  $\partial W/\partial I_1$  and the values of  $\partial W/\partial I_2$  for various values of  $I_2$  can be calculated as in §8. The value so obtained for  $\partial W/\partial I_1$  is  $1.45 \text{ kg./cm.}^2$ , and the calculated dependence of  $\partial W/\partial I_2$  on  $I_2$  is given in figure 20. From these values we can, in principle, calculate by means of equations (14.2) and (14.4) the  $M$  against  $\psi$  curves for various values of  $\lambda$ . However, the accuracy of the experimental results hardly justifies the numerical integrations involved and, instead, we shall calculate for each value of  $\lambda$  the value of  $M$  for  $\psi = 1.4$  radians/cm. by means of the approximation to equation (14.2)

$$M = \pi \psi a^4 \left[ \frac{\partial W}{\partial I_1} + \frac{1}{\lambda} \frac{\partial W}{\partial I_2} \right]_{r=a}. \quad (18.4)$$

The calculated values of  $M$  and those obtained from figure 19 are compared in table 11.

TABLE 11

$\lambda$	1.095	1.238	1.431	1.725	2.072
$[M]_{\psi=1.4}$ calculated	426	408	386	361	338
$[M]_{\psi=1.4}$ measured	400	400	375	350	325

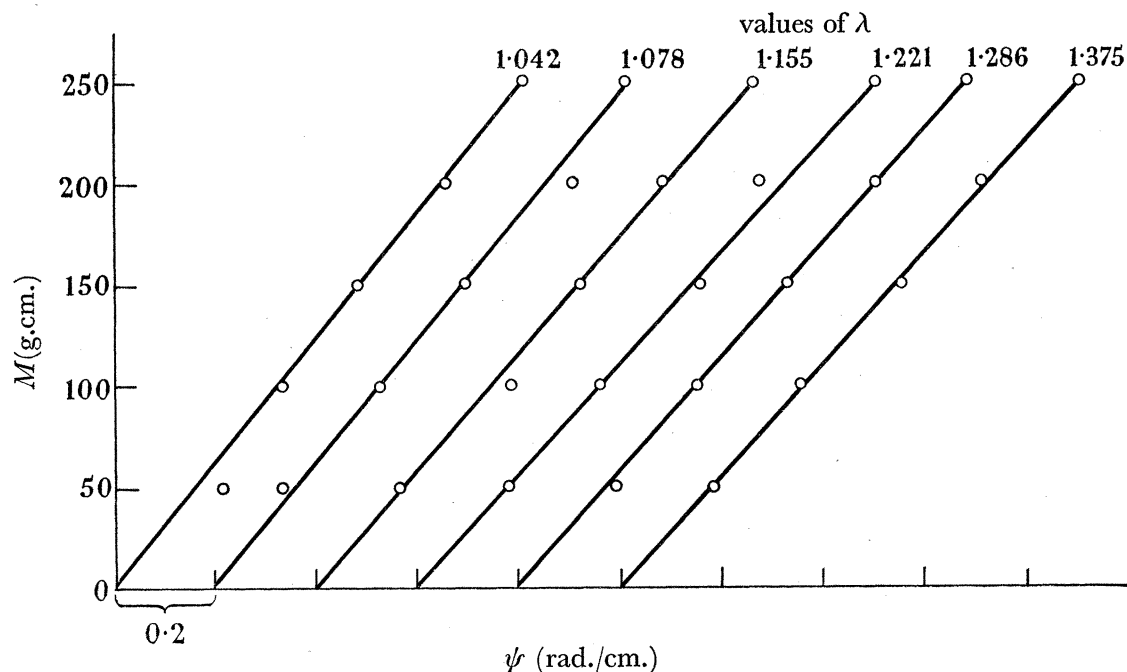


FIGURE 21. Plot of torsional couple  $M$  against amount of torsion  $\psi$  for various values of the extension ratio  $\lambda$  (small range of variation of  $\psi$ ; the origin is shifted by 0.2 unit parallel to the abscissa for each increment in the value of  $\lambda$ ).

It is not possible to test accurately the relation (14.5) using the experimental results given in figure 20 and table 10, owing to the inadequate number of experimental points for low values of  $\psi$ . Accordingly, measurements were made on another test-piece, prepared according to the same specification, of corresponding values of  $M$ ,  $N$  and  $\psi$  at various values of  $\lambda$  for values of  $\psi$  up to about 0.9 radian/cm. with the object of testing the relation (14.5). The  $M$  against  $\psi$  curves obtained are shown in figure 21 and the corresponding values of  $[N]_{\psi=0}$  and  $\lambda$  and of the values of  $[M/\psi]_{\psi=0}$  obtained from figure 21 are given in the first three rows

of table 12. The values of  $2(\lambda - 1/\lambda^2) [M/\psi]_{\psi=0}/a^2[N]_{\psi=0}$  calculated from these for each value of  $\lambda$  are given in the last row of the table and are seen to be in good agreement with the theoretically predicted value of unity.

TABLE 12

$\lambda$	1.042	1.078	1.155	1.221	1.286	1.375
$[N]_{\psi=0}$ (g.)	331	382	1080	1380	1725	2065
$[M/\psi]_{\psi=0}$ (g.cm. <sup>2</sup> )	306	300	286	276	280	272
$\frac{2(\lambda - 1/\lambda^2) [M/\psi]_{\psi=0}}{a^2[N]_{\psi=0}}$	0.99	0.99	0.98	0.98	0.98	0.99

## 19. DISCUSSION

It has been seen that, within the accuracy of the experiments, the load-deformation characteristics for a number of simple types of deformation of the rubber can be interpreted in terms of a single form for the stored-energy function  $W$ . This is such that  $\partial W/\partial I_1$  is independent of both  $I_1$  and  $I_2$ , that  $\partial W/\partial I_2$  is independent of  $I_1$  and falls with increase of  $I_2$ . This means that  $W$  is a function of the form

$$W = C(I_1 - 3) + f(I_2 - 3), \quad (19.1)$$

where  $C$  is a constant. It is, of course, possible that some other form of the stored-energy function would give equally good agreement with the experimental results, and that the differences between such a form and that which has been discussed would become apparent if other types of deformation were considered. For example, some slight dependence of  $\partial W/\partial I_2$  on  $I_1$  might well pass unnoticed in the series of experiments carried out. For, in the experiments on pure shear and simple torsion  $I_1 = I_2$  and in the experiments on simple extension or on pure shear or simple torsion superposed on a simple extension  $I_1$  increases with  $I_2$  and is not very different from it, so that a slight variation of  $\partial W/\partial I_2$  with  $I_1$  might very easily be interpreted, within the accuracy of the experiments, as a variation with  $I_2$ . Again, in the experiments on simple compression, the range of variation of  $I_2$  is so much greater than that of  $I_1$  that any variation of  $\partial W/\partial I_2$  with  $I_1$  may be masked.

In principle, the experiments on large pure homogeneous deformations (§§ 2 to 4) are not open to this ambiguity. In practice, however, the values of  $\partial W/\partial I_1$  and  $\partial W/\partial I_2$  obtained from them are so inaccurate, particularly at the lower values of  $I_1$  and  $I_2$ , that this theoretical advantage is largely lost. However, even though this possible ambiguity in the form for  $W$  must be admitted, it remains true that the various load-deformation relations considered can be interpreted, within experimental error, in terms of a single form for  $W$ .

The fact that this form for  $W$  is such that  $\partial W/\partial I_2$  is not zero represents a departure from the prediction of the kinetic theory of rubber-like elasticity which leads (Treloar 1943) to the expression

$$W = C(I_1 - 3), \quad (19.2)$$

in which  $C$  is a constant. This raises the question of the molecular mechanism which gives rise to the departure—a problem which will not be pursued here.

Much of the discussion of the individual experiments has been concentrated on the finer details of the experimental results, with the effect that certain broad features may have been obscured. For each type of deformation considered, the deforming forces are expressed in terms of the amount of deformation by expressions which consist of the product of two factors.

One of these depends only on the deformation, increases from zero as the deformation increases and is responsible for the major part of the variation of the load with deformation. The other depends on the stored-energy function and the dimensions of the test-piece as well as on the amount of deformation, and is responsible for relatively small modifications in the shape of the load-deformation curves. For example, in the case of pure shear it is seen from (5.2) that the first factor is  $2(\lambda - 1/\lambda^3)$ , where  $\lambda$  is the extension ratio in the direction of application of the load, while the second factor is  $A(\partial W/\partial I_1 + \partial W/\partial I_2)$ , where  $A$  is the cross-sectional area of the undeformed test-piece. It is seen from figure 9 that the total variation of the second factor is only about 15% over the whole range of the experiment.

#### D. APPENDICES

##### 20. APPENDIX 1. THE PREPARATION OF THE VULCANIZED RUBBER SPECIMENS

In all the experiments described in this paper one of two formulations was used for the preparation of the rubber test-pieces. These will be referred to as *A* and *B*.

###### *Vulcanized rubber A*

In the preparation of a test-piece of vulcanized rubber *A*, the mix employed was, in parts by weight: natural rubber (smoked sheet) 100, sulphur 3, zinc oxide 5, stearic acid 1, nonox 1, M.B.T. 0.5.

This mix was vulcanized at a temperature of 141°C for 45 min.

###### *Vulcanized rubber B*

In the preparation of vulcanized rubber *B*, the mix employed was, in parts by weight: natural rubber (smoked sheet) 100, sulphur 2, zinc oxide 2, stearic acid 0.5, nonox 0.5, M.B.T.S. 1.

This mix was vulcanized at a temperature of 141°C for 30 min.

In all cases the test specimens were made by a moulding process or were cut from specimens so made.

##### 21. APPENDIX 2. THE MOONEY FORM OF THE STORED-ENERGY FUNCTION

In this section it is shown that the Mooney form (1.3) for the stored-energy function must be valid for sufficiently small deformations of an ideal incompressible highly elastic material which is isotropic in its undeformed state.

The strain invariants  $I_1$  and  $I_2$  are given in terms of the principal extension ratios  $\lambda_1$ ,  $\lambda_2$  and  $\lambda_3$  by equation (1.1), and are subject to the restriction  $\lambda_1\lambda_2\lambda_3 = 1$  on account of the incompressibility of the material. We may write

$$\lambda_1 = 1 + e_1, \lambda_2 = 1 + e_2 \quad \text{and} \quad \lambda_3 = 1 + e_3. \quad (21.1)$$

Introducing expressions (21.1) into (1.1), we obtain, for  $e_1$ ,  $e_2$  and  $e_3$  less than unity,

$$\left. \begin{aligned} I_1 - 3 &= 2(e_1 + e_2 + e_3) + (e_1^2 + e_2^2 + e_3^2) \\ \text{and} \quad I_2 - 3 &= -2(e_1 + e_2 + e_3) + 3(e_1^2 + e_2^2 + e_3^2) - \dots \end{aligned} \right\} \quad (21.2)$$

Introducing the expressions (21.1) into the incompressibility condition  $\lambda_1\lambda_2\lambda_3 = 1$ , we obtain

$$(e_1 + e_2 + e_3) + (e_2e_3 + e_3e_1 + e_1e_2) + e_1e_2e_3 = 0. \quad (21.3)$$

Substituting in (21.2) from (21.3), we obtain

$$\left. \begin{aligned} I_1 - 3 &= (e_1 + e_2 + e_3)^2 - 4(e_2 e_3 + e_3 e_1 + e_1 e_2) + O(e^3) \\ \text{and} \quad I_2 - 3 &= 3(e_1 + e_2 + e_3)^2 - 4(e_2 e_3 + e_3 e_1 + e_1 e_2) + O(e^3) \dots \end{aligned} \right\} \quad (21.4)$$

in which  $O(e^3)$  represents terms of the third and higher degrees in  $e_1$ ,  $e_2$  and  $e_3$ . From (21.3), it is seen that  $(e_1 + e_2 + e_3)^2$  can be expressed as the sum of terms of the fourth and higher degrees in  $e_1$ ,  $e_2$  and  $e_3$ . Consequently,

$$\left. \begin{aligned} I_1 - 3 &= -4(e_2 e_3 + e_3 e_1 + e_1 e_2) + O(e^3) \\ \text{and} \quad I_2 - 3 &= -4(e_2 e_3 + e_3 e_1 + e_1 e_2) + O(e^3). \end{aligned} \right\} \quad (21.5)$$

Therefore, if  $e_1$ ,  $e_2$  and  $e_3$  are sufficiently small so that in the general expression (1.2) for the stored-energy function, into which the expressions (21.5) for  $(I_1 - 3)$  and  $(I_2 - 3)$  are introduced, terms of higher degree than the third in  $e_1$ ,  $e_2$  and  $e_3$  may be neglected, we obtain the Mooney expression (1.3) for the stored-energy function. This expression is the equivalent for an incompressible material of the second order approximation stored-energy function derived by Murnaghan (1937) for a compressible material.

## 22. APPENDIX 3. PRELIMINARY EXPERIMENT ON THE METHOD OF MEASURING THE FORCES IN THE EXPERIMENTS ON PURE HOMOGENEOUS DEFORMATION

In the experiments on pure homogeneous deformation (§3) five strings were attached to each side of the square sample shown in figure 3. The deformation of the sample was measured over the central nine elements of the ruled grid, and the forces maintaining the deformation were taken as the average of the tensions measured in the three central strings of appropriate sides.

In a preliminary experiment the tensions in all five strings on two adjacent sides were measured for one series of measurements at  $I_1 = 11$ . In table 13 the stresses  $t'_1$  and  $t'_2$  per unit area of deformed section perpendicular to their direction computed from an average of the measured tensions in all five strings are compared with the corresponding stresses  $t_1$  and  $t_2$  computed from the average of the measured tensions in the central three strings.

We see that in general  $t'_1$  and  $t'_2$  are only some 2 to 4 % greater than  $t_1$  and  $t_2$ . It seems therefore that the forces on the outer lugs are not sufficiently different from those on the central lugs radically to affect the computed stress values. In view of these small deviations the assumption that the stresses over the uniformly strained central nine elements are defined by the forces on the central three strings of each side, and are not affected by the stresses in the inhomogeneously deformed peripheral area, cannot lead to large errors.

TABLE 13

$\lambda_1$	2.80	2.70	2.60	2.50	2.40
$\lambda_2$	1.76	1.91	2.05	2.18	2.28
$t_1$ (kg./cm. <sup>2</sup> )	31.8	29.1	27.2	25.4	23.7
$t'_1$ (kg./cm. <sup>2</sup> )	32.8	30.5	28.2	26.2	24.3
$t_2$ (kg./cm. <sup>2</sup> )	15.7	17.5	19.7	21.1	22.0
$t'_2$ (kg./cm. <sup>2</sup> )	15.6	18.0	20.2	22.2	23.2



23. APPENDIX 4. THE LINEARITY OF THE RELATION BETWEEN  
 $[\partial W/\partial I_1 + (1/\lambda) \partial W/\partial I_2]$  AND  $1/\lambda$  FOR SIMPLE EXTENSION

It has been seen that if the dependence of  $[\partial W/\partial I_1 + (1/\lambda) \partial W/\partial I_2]$  on  $1/\lambda$  is measured, under conditions for which  $I_1$  and  $I_2$  are given by

$$I_1 = \lambda^2 + \frac{2}{\lambda} \quad \text{and} \quad I_2 = \frac{1}{\lambda^2} + 2\lambda, \quad (23\cdot1)$$

either by experiments on simple extension (§ 10) or by experiments on torsion superposed on simple extension (§ 18), a linear relation is obtained between the two quantities. It has already been pointed out (§ 10) that this might lead one to conclude that  $\partial W/\partial I_1$  and  $\partial W/\partial I_2$  are substantially constant over the range of values of  $I_1$  and  $I_2$  considered, and that such a conclusion would be out of accord with results of other experiments. It has been seen that the experimental results are better interpreted in terms of a form for  $W$  such that  $\partial W/\partial I_1$  is constant and  $\partial W/\partial I_2$  varies with  $I_2$  only. It can be shown analytically that such a form for  $W$  may easily give rise to an apparently linear relation between  $[\partial W/\partial I_1 + (1/\lambda) \partial W/\partial I_2]$  and  $1/\lambda$ , over the range of  $1/\lambda$  covered by the experiments, when  $I_1$  and  $I_2$  are given by (23·1).

If  $\partial W/\partial I_1$  is constant ( $= C$ , say) and  $\partial W/\partial I_2$  is a function of  $I_2$  only, we can write

$$\frac{\partial W}{\partial I_1} + \frac{1}{\lambda} \frac{\partial W}{\partial I_2} = C + \frac{1}{\lambda} \sum_{i=0}^{\infty} C_i \left( \frac{1}{\lambda^2} + 2\lambda - 3 \right)^i. \quad (23\cdot2)$$

If over the range of values of  $(I_2 - 3)$  considered,  $C_i (i > 1)$  are sufficiently small that second and higher degree terms in (23·2) can be neglected, we obtain from (23·2)

$$\frac{\partial W}{\partial I_1} + \frac{1}{\lambda} \frac{\partial W}{\partial I_2} = (C + 2C_1) + \frac{1}{\lambda} (C_0 - 3C_1) + \frac{C_1}{\lambda^3}. \quad (23\cdot3)$$

We see that the inclusion in (23·2) of the first-degree term in  $(1/\lambda^2 + 2\lambda - 3)$  does not greatly affect the linearity of the relationship between  $[\partial W/\partial I_1 + (1/\lambda) \partial W/\partial I_2]$  and  $1/\lambda$ , for  $1/\lambda$  in the range 0·9 to 0·4, provided that  $C_1$  is not too large compared with  $C$  or  $C_0$ . If the apparent linearity were interpreted as implying that  $\partial W/\partial I_1$  and  $\partial W/\partial I_2$  are constant and the ratio  $(\partial W/\partial I_2)/(\partial W/\partial I_1)$  were calculated on this basis, it is seen that if  $C_1$  is negative a value greater than  $C_0/C$  would be obtained. It will, of course, be appreciated that the small departure from linearity due to the term  $C_1/\lambda^3$  in (23·3) may be compensated by the effect of higher degree terms in (23·2).

24. APPENDIX 5. FURTHER REMARKS ON THE RESULTS OF THE SIMPLE  
 COMPRESSION EXPERIMENT

In § 13, the values of  $\partial W/\partial I_1$  and  $\partial W/\partial I_2$ , and hence of the ratio  $(\partial W/\partial I_2)/(\partial W/\partial I_1)$ , have been calculated from figure 14 over a wide range of values of  $I_2$  on the assumption that they are all independent of  $I_1$  and that  $\partial W/\partial I_1$  is also independent of  $I_2$ . The assumption was also made that  $(\partial W/\partial I_2)/(\partial W/\partial I_1)$  has the value 0·16 when  $I_2 = 4\cdot25$ . All these assumptions derive from the results of earlier experiments which were, however, carried out on rubber test-pieces prepared according to a somewhat different recipe from those with which the results given in figure 14 were obtained.

In view of this, it appears desirable to investigate the effect on the calculated values of  $(\partial W/\partial I_2)/(\partial W/\partial I_1)$  at other values of  $I_2$  of choosing somewhat different values at  $I_2 = 4\cdot25$ .



The results of these calculations are given in table 14. The value of  $(\partial W/\partial I_2)/(\partial W/\partial I_1)$  at  $I_2 = 4.25$  is denoted by  $\alpha$ . It is seen that the assumed value for  $\alpha$  has relatively little effect on the values calculated for  $(\partial W/\partial I_2)/(\partial W/\partial I_1)$  at the low and high values of  $I_2$ .

TABLE 14

$\alpha$	$I_2$	3.14	3.35	3.69	4.25	9.67	25.4	49.3	81.2
0.06		0.32	0.26	0.17	0.06	0.10	0.032	0.026	0.030
0.11	$\frac{\partial W/\partial I_2}{\partial W/\partial I_1}$	0.35	0.30	0.22	0.11	0.12	0.036	0.031	0.033
0.16		0.39	0.34	0.26	0.16	0.13	0.040	0.033	0.035
0.21		0.43	0.38	0.31	0.21	0.14	0.045	0.037	0.038
0.26		0.47	0.42	0.35	0.26	0.15	0.049	0.041	0.042

This work forms part of a programme of research undertaken by the Board of the British Rubber Producers' Research Association. Our thanks are due to Dr G. Gee and Dr L. R. G. Treloar for valuable discussions and advice.

## REFERENCES

- Mooney, M. 1940 *J. Appl. Phys.* **11**, 582.  
 Murnaghan, F. D. 1937 *Amer. J. Math.* **59**, 235.  
 Rivlin, R. S. 1947 *J. Appl. Phys.* **18**, 444.  
 Rivlin, R. S. 1948a *Phil. Trans. A*, **240**, 459.  
 Rivlin, R. S. 1948b *Phil. Trans. A*, **240**, 491.  
 Rivlin, R. S. 1948c *Phil. Trans. A*, **240**, 509.  
 Rivlin, R. S. 1948d *Phil. Trans. A*, **241**, 379.  
 Rivlin, R. S. 1949a *Proc. Roy. Soc. A*, **195**, 463.  
 Rivlin, R. S. 1949b *Phil. Trans. A*, **242**, 173.  
 Treloar, L. R. G. 1943 *Trans. Faraday Soc.* **39**, 241.  
 Treloar, L. R. G. 1944 *I.R.I. Trans.* **19**, 201.  
 Treloar, L. R. G. 1948 *Proc. Phys. Soc.* **60**, 135.